Dynamics of the Ocean Surface in the Polar and Subpolar North Atlantic over the last 500 000 Years

Dynamik der Ozeanoberfläche im polaren und subpolaren Nordatlantik während der letzten 500 000 Jahre

---

Evguenia S. Kandiano

Ber. Polarforsch. Meeresforsch. 456 (2003)
ISSN 1618 - 3193

Evguenia S. Kandiano

GEOMAR Forschungszentrum für Marine Geowissenschaften
Wischhofstraße 1-3
24148 Kiel, Bundesrepublik Deutschland

Die vorliegende Arbeit ist die inhaltlich unveränderte Fassung einer Dissertation, die 2002 an der mathematisch-naturwissenschaftlichen Fakultät der Christian-Albrechts-Universität zu Kiel vorlag.

Abstract

This study represents a multiproxy reconstruction of the ocean surface temperatures (SST) and surface water circulation in the polar and subpolar North Atlantic during the last 500,000 years (marine isotope stages 1-13). Two cores were selected for this aim, one from the Rockall Plateau and one from the Nordic seas. Foraminiferal diversities are used as the main paleoceanographic tool for paleotemperature determinations. They are compared with planktic and benthic stable isotope measurements, results of Mg/Ca thermometry as well as iceberg-rafted debris (IRD) records.

To obtain paleotemperature estimates in the North Atlantic both Modern Analogue Technique (MAT) and Transfer Function Technique (TFT) were applied. SSTs reveal glacial-interglacial as well as persistent millennial-scale variability over the entire investigated period. During the last five glacial-interglacial cycles, interglacial climate conditions exhibit some differences. Warmest conditions are found for marine isotope stage (MIS) 5.5 and MIS 11, whereas the Holocene and MIS 13 are about 2°C colder. Interglacial peak temperature during MIS 7 and MIS 9 reach the same value as during the Holocene, however, enhanced dissimilarity coefficients for MIS 7 derived from MAT indicate that the obtained temperature results may significantly deviate from real values. Results of detailed faunal analysis imply that SSTs during MIS 7 are largely overestimated.

In the North Atlantic, millennial-scale variability is strongly reduced in amplitude during peak interglaciations which is coincident with cessation of IRD input. During glacial and interstadial times short-lived climatic fluctuations retain their regular sequence of events. Every short-lived cycle begins with a slight initial cooling followed by further considerable temperature decrease, coincident with a peak in IRD deposition, and ends in abrupt warming which brings the climate conditions to the initial state. IRD events reveal striking differences in both frequency and intensity depending on the particular climate mode. Periods with pronounced climate contrasts, such as MIS 6, are marked by highest and frequent IRD input whereas frequency and intensity are considerably reduced during times characterized by less climate contrasts, such as MIS 7-9.

In the Nordic seas foraminiferal diversities in different mesh-size fractions were investigated for the time interval of the later part of MIS 8 into early MIS 7 and the last 30 cal. ka to select the most representative fraction for paleoceanographic applications. Selected time intervals cover periods with different climatic conditions: the last glacial maximum (LGM), which represents severe cooling, the Holocene, the pronounced interglaciation, and MIS 7-8, a period with reduced climatic contrasts. The obtained results show that changes in foraminiferal diversities in the larger size fraction (125-250 µm, 150-500 µm), which is conventionally used, occur only during warm extremes, such as the Holocene, whereas during other periods foraminiferal assemblages remain almost monospecific, mainly represented by polar species *Neogloboquadrina pachyderma* sinistral (s). By contrast, the smaller size fractions (80-100 µm, 100-150 µm) exhibit considerable increase of the subpolar species *Turborotalita quinqueloba* which makes it possible to trace inflow of Atlantic water into the Nordic seas and to reconstruct sea surface properties and surface ocean circulation also during glacial and interstadial times.

Zusammenfassung

In dieser Arbeit wurden mit Hilfe unterschiedlicher Parameter die Meeresoberflächentemperatur (MOT) und die Oberflächenwasserzirkulation im polaren und subpolaren Nordatlantik während der letzten 500.000 Jahre (marine Isotopenstadien 1-13) rekonstruiert. Zu diesem Zweck wurden zwei Kerne ausgewählt, je einer vom Rockall-Plateau und aus der Norwegisch-Grönländischen See. Die Zusammensetzung der Foraminiferen wird als paläo-ozeanographisches Hauptwerkzeug für die Bestimmung der Paläotemperatur genutzt. Sie wird mit Messungen planktischer und benthischer stabiler Isotope, Ergebnissen von Mg/Ca-Thermometrie sowie Aufzeichnungen des eisbergverfrachteten terrigenen Materials (ETM) verglichen.

Um die Paläotemperatur im Nordatlantik abzuschätzen, wurden sowohl die Moderne Analog-Technik (MAT) als auch die Transferfunktionstechnik (TFT) angewendet. MOTs ergeben die Variabilität im glazial-interglazialen Maßstab sowie im Maßstab von Jahrtausenden für die gesamte untersuchte Zeitspanne. Während der letzten fünf glazial-interglazialen Zyklen zeigen die interglazialen Klimabedingungen einige Unterschiede. Die wärmsten Bedingungen sind für das marine Isotopenstadium (MIS) 5.5 und MIS 11 zu finden, wohingegen das Holozän und MIS 13 um etwa 2°C kälter sind. Die interglaziale Höchsttemperatur während MIS 7 und MIS 9 erreicht denselben Wert wie während des Holozäns; erhöhte Abweichungskoeffizienten für MIS 7, die sich durch MAT ergeben, zeigen jedoch, dass die erhaltenen Temperaturergebnisse beträchtlich von den wirklichen Werten abweichen können. Ergebnisse der eingehenden Faunenanalyse implizieren, dass die MOTs während MIS 7 weitgehend überschätzt werden.

Im Nordatlantik ist die Amplitude der Variabilität im Jahrtausendmaßstab während maximaler Interglazialräume stark reduziert, was mit einer Unterbrechung im ETM-Eintrag zusammenfällt. In glazialen und interglazialen Zeiten bleiben kurzzeitige Klimafluktuationen in ihrer regelmäßigen Abfolge erhalten. Jeder kurzzeitige Zyklus beginnt mit einer leichten anfänglichen Abkühlung, die von einem weiteren beträchtlichen, gleichzeitig mit einem Maximum an ETM-Ablagerung zusammenfallenden Temperaturrückgang gefolgt wird, und endet mit einer unvermittelten Erwärmung, die die Klimabedingungen zu ihrem Anfangszustand zurückführt. ETM-Ereignisse zeigen dabei Unterschiede sowohl in der Häufigkeit als auch in der Intensität, je nach den betreffenden Klimaverhältnissen. Zeiträume mit ausgeprägten Klimaunterschieden, wie MIS 6, sind durch höchsten und häufigen ETM-Eintrag gekennzeichnet, wohingegen die Häufigkeit und Intensität zu Zeiten, die von weniger starken Klimaunterschieden gekennzeichnet sind, wie MIS 7-9, beträchtlich herabgesetzt sind.

In der Norwegisch-Grönländischen See wurde die Zusammensetzung der Foraminiferen in unterschiedlichen Korngrößenfraktionen für die Zeitspanne des späten MIS 8 bis ins frühe MIS 7 und für die letzten 30 cal ka detailliert untersucht, um die repräsentativste Fraktion für paläo-ozeanographische Anwendungen zu erhalten. Die ausgewählten Zeitspannen decken Perioden mit unterschiedlichen Klimabedingungen ab: das Letzte Glaziale Maximum (LGM), das eine starke Abkühlung repräsentiert, das Holozän, den ausgeprägten Interglazialraum, und MIS 7-8, eine Zeitspanne mit abgeschwächten Klimaunterschieden. Die erhaltenen Resultate zeigen, dass Veränderungen in der

Zusammensetzung der Foraminiferen in den üblicherweise verwendeten größeren Fraktionen (125-250 µm bzw. 150-500 µm) nur während extremer Warmzeiten wie dem Holozän auftreten. Dagegen bleiben Foraminiferengesellschaften zu anderen Zeiten fast monospezifisch, wobei sie hauptsächlich von der polaren Art *Neogloboquadrina pachyderma* sinistral (s) repräsentiert werden. Im Gegensatz dazu zeigen die kleineren Fraktionen (80-100 µm, 100-150 µm) einen beträchtlichen Anstieg des Anteils der subpolaren Art *Turborotalita quinqueloba*. Diese Erkenntnis ermöglicht, den Eintrag von Atlantikwasser in den polaren Nordatlantik auch für die Zeitintervalle zu rekonstruieren, die nicht von den Meeresoberflächeneigenschaften extremer Warmzeiten geprägt wurden.

1. Introduction

1.1. Main objectives

The Late Cenozoic closure of the seaway between the North and South America 4.6 million years ago intensified the Gulf Stream. This brought saline water masses to higher latitudes, which promoted a new reorganization of the world ocean circulation (Haug and Tiedemann, 1998). Since this time, major changes in climate, regulated by alterations in eccentricity, obliquity and precession of the Earth, have provoked global-scale glacial-interglacial fluctuations (Hays et al., 1976). During warm episodes like today, northward heat transport maintains global ocean thermohaline circulation, ameliorating temperatures over North-Western Europe. Warm Atlantic waters reach as far north as the Nordic seas where they gain unusually high density, resulting from cooling, and sink to the abyss. During colder periods such as glaciations the strengths of Gulf Stream waters were reduced due to lowered salinity in high-latitude surface waters that in turn results from decreased evaporation. As a consequence thermohaline circulation and thus deep water formation in the polar North Atlantic, is considerably weakened or completely shut down (Broecker and Denton, 1990; Broecker, 1991). It is generally believed that without this deep water production warm water masses could not penetrate far north, indeed, during glacial periods they were mainly restricted to the mid-latitudes (McIntyre et al.,1972; Chapman and Maslin, 1999). Thus, the most remarkable feature of the Quaternary climate system is the development of glacial-interglacial as well as millennial-scale climate oscillations.

This short-lived abrupt climatic changes, first discovered in the Greenland ice cores (e.g. Johnsen et al., 1992; Grootes et al., 1993; Grootes and Stuvier, 1997), are superimposed on the general glacial-interglacial trend. Although, the most pronounced millennial-scale fluctuations have been registered in the North Atlantic region (e.g. Bond et al., 1997, Chapman et al., 2000; Maslin and Shackleton, 1995), there is growing evidence that these climate oscillations occurred also on a global scale (Lowell et al., 1995; Blunier et al., 1998; Schulz et al., 1998; de Menocal et al., 2000; Hüls and Zahn, 2000). In the North Atlantic marine sediments the most severe cooling events, so-called

Heinrich events, which are attributed to culmination episodes of millennial-scale climatic fluctuations, result from circum-North-Atlantic ice sheet collapses. During Heinrich events a large freshwater input released from melting icebergs, prevents deep water production and shuts down thermohaline Atlantic circulation, leading to a further climatic cooling. These events are therefore also recognizable by enhanced iceberg-rafted debris (IRD) deposition and considerable depletions in planktic foraminiferal $\delta^{18}O$ as well as records by abrupt sea surface temperature (SST) decreases (Heinrich, 1988; Bond and Lotti, 1995; Elliot et al., 1998; van Kreveld et al., 2000).

Therefore, changes in the thermohaline ocean circulation in the North Atlantic is regarded a key mechanism which might amplify an initial climatic signal (e.g. Broecker, 1994; Rahmstorf, 1994, 1996; Paillard and Cortijo, 1999). Once an equilibrium between temperature and salinity of surface waters of one of climatic mode is distorted, this immediately provokes changes in thermohaline Atlantic circulation which then causes further climate changes (e.g. Seidov and Maslin, 1999; Ganopolski and Rahmstorf, 2001; Maslin et al., 2001). Thus, to get insights of climate driving mechanisms the accurate estimates of past sea surface properties are needed. In this regard SST determination seems to be a most useful investigative target. To estimate paleoSSTs a number of proxies is available. Along with elaborated methods based on variations in faunal diversities or oxygen isotope composition of planktic foraminifers, new chemical methods including SST estimations derived from changes in Mg/Ca ratio in foraminiferal tests are available now.

Understanding the principals of interactions between glacial-interglacial and short-lived climate fluctuations is extremely important for climate prediction in general. Thus, answers to the following questions are of major relevance:

- Did short-lived climate fluctuations persist invariably throughout the last 500,000 years?
- Did their pattern change in relation to differences in glacial and interglacial temperature amplitudes?

These questions were not adequately answered so far since more recent investigations mainly concentrated on climate reconstructions of the last glacial-interglacial cycle. The

few available long quantitative SST records that were obtained from the North Atlantic (Ruddiman and McIntyre, 1976; Ruddiman et al., 1986a, b; Ruddiman and Esmay, 1987) need to be reassessed regarding to both glacial-interglacial variability and millennial-scale variability. As established by previous researchers interglacial climate similarity in the North Atlantic during the last five glacial-interglacial cycles (Ruddiman and McIntyre, 1976; Ruddiman et al., 1986a, b) seems to be peculiar since in other regions interglacial conditions considerably differ between each other (Bauch, 1997; Lyle et al., 2001). In addition, they were of insufficient resolution to trace short-term climate fluctuations. Evidence of millennial-scale climate variability in the North Atlantic from periods older than 135,000 years is therefore scarce and represented by only few fragmentary data (Oppo and Lehmann, 1995; Oppo et al., 1998; McManus et al.,1999; Niscott et al., 2001). To answer the problems mentioned above, this study focuses on SST reconstructions derived from changes in foraminiferal diversity in the North Atlantic during the last 500,000 years and on an assessment of a new approach of qualitative SST estimations for the Nordic seas using small-sized foraminiferas to trace Atlantic water input. Alterations of foraminiferal diversity precisely reflect temperature fluctuations since these surface dwelling microorganisms are adopted to relatively narrow temperature ranges (Bé and Tolderlund, 1971; Barash, 1988). In areas with good carbonate preservation, such as the North Atlantic, they are a good mean to reconstruct sea surface temperatures, thus being useful to trace both glacial-interglacial and millennial-scale variability. The interpretation of the derived temperature estimates is supported by IRD and $\delta^{18}O$ records obtained by previous researchers (Helmke and Bauch, 2001; Didié et al., 2002). SST results from the North Atlantic are also compared with temperature estimates derived from Mg/Ca measurements in *Globigerina bulloides* (Müller, 2000) in order to assess the paleoclimatic perspectives of the newly developed method in this region.

As it was already discussed, the deep water production which initiates global thermohaline ocean circulation occurs in the present time in the Nordic seas. To get better insights of climatic dynamics it is important to investigate in detail changes in sea surface properties in this region. However, the Nordic seas SST determinations derived from foraminiferal census counts are complicated by low foraminiferal diversity, at least in the commonly used size fraction >150 µm. On the base of conventional counting procedures only strong glacial-interglacial contrasts are recognizable in foraminiferal

records in this region (Kellogg, 1976, 1977, 1980; Bauch, 1997) whereas temperature fluctuation characterized by diminished amplitudes remain poorly investigated due to lack of serviceable paleoceanographic tools. This work therefore also attempts to solve the following problem:

- How can short-lived climate fluctuations be traced in the Nordic seas region during glacial and interstadial periods?

As it was already indicated by previous studies, the content of subpolar foraminiferal species in size fractions <150 μm seems to be surprisingly increased in the polar region during glacial times (Marquard and Clark, 1987; Bauch, 1994; Hebbeln et al., 1994; Dokken and Hald, 1996). But because of apparent complications with taxonomy when counting small-sized specimens (Kellogg, 1984), this method was not broadly employed by researchers so far. In this study foraminiferal diversities in different mesh-size fractions were carefully examined to assess the usability of small-sized fractions for paleoceanographical reconstructions.

1.2. Oceanographic settings of the investigated area and position of selected core sites

Hydrography of the investigated region is mainly defined by the influence of warm surface waters of the North Atlantic Drift that flow into the Norwegian seas as the Norwegian Current (Fig. 1.1). This warm and high saline waters of the Norwegian Current and cold, low saline waters of the East Greenland Current (EGC), advected from the adjacent Arctic region, form the Atlantic and the Polar domains, respectively. These two domains are separated by waters of the Arctic domain which are characterized by high temperature and salinity gradients (Levitus and Boyer, 1994). Oceanographic boundaries between the domains are also well recognizable in marine surface sediments by changes in foraminiferal abundances and total calcium carbonate content (Johannessen et al., 1994). The Arctic Domain is considered to be the main location of deep water formation in the Nordic seas (McCave and Tucholke, 1986; Ganopolski and Rahmstorf, 2001). Here saline Atlantic waters gain high density due to cooling and sink to the abyss which gives initial impulse to the global ocean conveyor (Broecker and Denton, 1990). This deep water mass is then advected into the North

Atlantic over the Greenland-Scotland ridges where it mixes with Labrador Sea Water (LSW) and Mediterranean Overflow Water (MOW) to form the North Atlantic Deep Water (NADW). NADW in turn is underlain by modified Antarctic Bottom Water (AABW), characterized by lower temperatures (Manighetti and McCave, 1995). NADW protrudes southward, mixes with deep waters from different sources on its way along the Antarctic continent and reaches the Pacific where this deep water is exposed to the surface again due to upwelling processes. Then it returns but as surface current to the North through the Caribbean Sea where it gains high salinity due to strong evaporation (Broecker, 1991). This overturning process maintains itself until the equilibrium between temperature and salinity is distorted due to influence of external factors. It is believed that during interglacial-glacial transitions the location of NADW production gradually migrated further south (Ganopolski and Rahmstorf, 2001; Sarnthein et al., 2001) whereas during Heinrich events it is completely shut down due to the low salinity meltwater cover that results from massive iceberg melting.

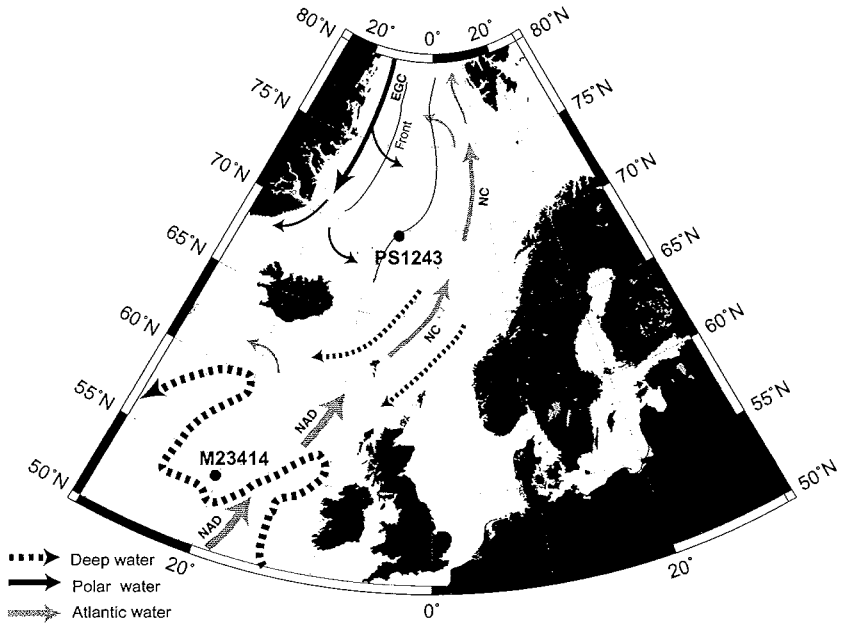

Fig. 1.1. Generalized present ocean circulation and locations of the investigated core sites; EGC – East Greenland Current, NAD – North Atlantic Drift, NC – Norwegian Current.

1.3. Foraminifera as a proxy for paleoceanography

Planktic foraminifera comprise a cosmopolitan group of sea-dwelling protozoa which is ascribed to the zooplankton. Their habitat is mainly restricted to the upper hundred meters of the ocean, although some species descend during their life cycle as deep as the first thousand meters (Bé and Tolderlund, 1971; Bé, 1977; Hemleben et al., 1989). They are ubiquitously distributed in the world ocean and have been found even in the ice-covered polar regions (Marquard and Clark, 1987; Bauch, 1999). The main characteristic feature of these organisms is calcite tests that sink to the bottom after death contributing substantially to pelagic sedimentation. These fossils were mainly used as biostratigraphic markers until Schott (1935) has introduced quantitative counts of foraminifera species within fossil assemblages demonstrating that down core changes in species compositions relate to glacial-interglacial variability. This finding provided a theoretical base for numerous further investigations and helped to develop quantitative approaches for paleotemperature estimations.

1.3.1. Paleotemperature estimates based on changes in foraminiferal diversity

The usability of Foraminifera as late Quaternary temperature markers is based on two assumptions:

1. Most of foraminiferal species are adopted to a narrow temperature range.
2. This group did not undergo significant evolutionary changes and changes in ecological preferences during late Quaternary times.

Therefore, using the principle of uniformitareanism it can be assumed that similar foraminiferal assemblages correspond to similar SSTs. Thus, paleoSSTs can be estimated by comparing fossil foraminiferal assemblages with the modern data.

For the first time, the relation between foraminiferal diversity and SST was quantitatively formalized by Imbrie and Kipp (1971). Their approach, the "Transfer Function Technique" (TFT), represents a factor regression. In this method, modern foraminiferal diversity is subdivided into several idealized end-member assemblage (factors). Each foraminiferal sample of the modern data base is expressed as a mixture

of factor loadings. These loadings are regressed against modern SST data base. PaleoSSTs can then be estimated by the established equation.

Another method, "Modern Analogue Technique" (MAT), was originally introduced by Hutson (1980) and further developed by Prell (1985). This method is based on direct comparison of a fossil foraminiferal assemblage of a given sediment sample with foraminiferal assemblages of the modern data base. PaleoSSTs are estimated as a mean of modern SSTs that correspond to the most similar modern assemblages, so-called best analogues.

Both of these methods are dependent on the used reference data base. Comparison of SST estimates obtained by both methods show little differences when they are based on the same data base (Ortiz and Mix, 1997; Hüls and Zahn, 2000). The precision in modern calibration is quite high in the middle temperature range. However, some problems of temperature estimates arise at the cold extreme due to reduction of the foraminiferal diversity to only one species *Neogloboquadrina pachyderma* sinistral (s). This species strongly dominates the assemblage in regions with summer temperatures below 5°C (Pflaumann et al., 1996), which makes SST estimates imprecise. So other approaches are needed to elaborate paleotemperature methods for the polar region, especially for periods other than peak interglaciations when species numbers are low.

1.4. Material and methods

1.4.1. Geographical position and stratigraphy of the investigated sediment cores

Both cores, selected for this study, underlay surface waters that are strongly affected by warm water advection and should bear signals of changes in sea surface properties initiated by alterations in thermohaline circulation (Fig. 1.1, 1.3; Table 1.1). Any migrations of oceanographic fronts that occurred during past climatic oscillations should be defined by changes in faunal diversity. Moreover, since both core sites are situated well above the lysocline, the sediments are not affected by dissolution thus showing good preservation of fossil calcareous assemblages. Core M23414-6/7/9 was recovered during "METEOR" cruise M17/2 from the Rockall area from underneath the North Atlantic Drift.

Table 1.1. Geographical position and water depth of the investigated sediment cores.

Core	Latitude	Longitude	Water depth, m	Reference
M23414-6 (B)	53.537 °N	20.537 °W	2201	Suess and Altenbach, 1992
M23414-8 (P)	53.538 °N	20.292 °W	2199	-"-
M23414-9 (G)	53.537 °N	20.288 °W	2196	-"-
PS1243-1 (G)	69.371 °N	06.540 °W	2710	Augstein et al., 1984
PS1243-2 (B)	69.375 °N	06.540 °W	2716	-"-

B - box core, G - gravity core, P - piston core

Core PS1243-1/2 was taken during "POLARSTERN" cruise ARK II/5 in 1984. This core site is located on the eastern slope of the Iceland Plateau within the modern pelagic sedimentation regime of the Nordic seas. The cores M23414 and PS1243 have already been appropriately spliced and sampled. The stratigraphy of both investigated cores has been well established in previous studies. The stratigraphic subdivision of the core M23414 is based on the 1 cm-step lightness records provided by Helmke and Bauch (2001), detailed planktic $\delta^{18}O$ records (Helmke and Bauch, submit.) and AMS radiocarbon measurements (Didié et al., in press) as well as assignment of the well-established ages of Heinrich events (Helmke et al., 2002).

The stratigraphic subdivision of core PS1243 was established in previous investigations on the base of $\delta^{18}O$ measurements performed on the planktic foraminifera *N. pachyderma* (s) and AMS radiocarbon dates (Bauch, 1997; Bauch et al., 2001a). The core section containing marine oxygen isotope stage (MIS) 8 to 7.5, a glacial-interglacial transition followed in the Nordic seas by temperate warming, was selected as a case study to find the optimal foraminiferal size fraction that most sensitively records Atlantic surface water input. The results of this case study were tested against the well-investigated upper section of the core that covers the last 30,000 years. The existing age model was slightly improved due to additional $\delta^{18}O$ isotope analysis which narrowed the resolution to 1 cm for the interval MIS 7-8.

1.4.2. Sample treatment

Faunal analyses of the investigated cores were carried out with different sample resolutions, which, however, allowed a detailed millennial-scale paleoceanographic reconstruction (Fig. 1.2).

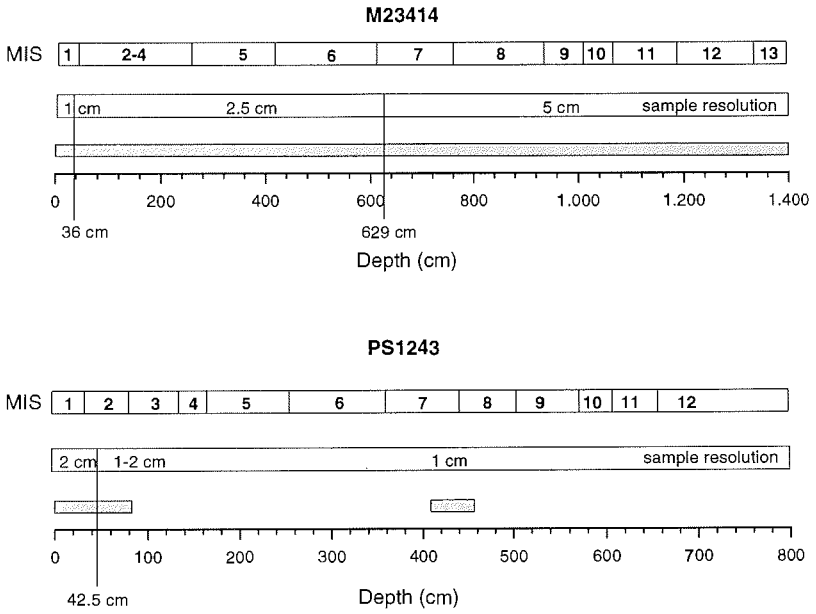

Fig. 1.2. Scheme demonstrating sample resolution of the faunal analysis of the investigated cores; Marine oxygen isotope stages (MIS) are indicated; gray bars show investigated parts of the cores.

All samples were treated according to conventional procedures. Before analysis processing they were freeze-dried, then washed over a 63 µm sieve, before dry-sieved into subfractions.

Faunal analyses were supported by planktic $\delta^{18}O$ isotope, carbonate content and IRD records derived from the same samples. These supplementary data were mainly provided by previous investigations (Jung, 1996; Didié, et al., 2002; Helmke and Bauch, 2001; Helmke et al., 2002). Additional planktic stable isotope measurements for core PS1243, performed within this study, are listed in the appendix (Table A.13). They were carried out on the polar foraminiferal species *N. pachyderma* (s) using a MAT 251 mass spectrometer; 25-30 four-chambered specimens from the 125-250 µm size fraction were selected for each analysis.

1.4.3. Faunal analysis

A total of 568 samples were considered by faunal analysis and 21 planktic foraminiferal species and morphotypes were distinguished. Taxonomy followed the species concept of Bé (1977), Saito et al. (1981), Kennett and Srinivasan (1983), and Hemleben et al. (1989). Intergrades between *Neogloboquadrina pachyderma* dextral (d) and *Neogloboquadrina dutertrei* were ascribed to *N. pachyderma* (d) following the strategy of Pflaumann et al. (1996). Foraminiferal census counts for the investigated cores are represented in percentages in the appendix (Table A.1, A.4-A.10)

North Atlantic (core M23414)

Following the convention of the CLIMAP Group (CLIMAP MEMBERS, 1976), planktic foraminiferal census counts were carried out on the >150 µm size fraction. All samples were subdivided into two subfractions 150-150 µm and >250 µm. Each subfraction was split by means of a microsplitter to 150-300 specimens and counted. Relative abundances of the species were recalculated using split factors. A minimum of 300 specimens in total was counted per sample.

Nordic seas (PS1243)

To find the optimal mesh size limit for foraminiferal counts with paleoceanographic implications, foraminiferal relative abundances were determined separately on the size fractions 80-150 µm, 100-150 µm, 125-250 µm, 150-500 µm for time interval MIS 8-7.5.

For the interval MIS 2-1 the size fractions 80-150 µm, 125-250 µm, and 150-500 µm were compared. Each fraction was split down to approximately 300 specimens.

To obtain control on dissolution, which is extremely important when working with small-sized fractions that partly consist of juvenile tests, the ratio between complete tests and fragments in the fraction 150-500 µm was considered (Table A.12, A.12).

1.4.4. Data treatment

To achieve a better control on temperature estimates, results of foraminiferal census counts from the North Atlantic core M23414 were treated with two different methods MAT (Prell, 1985) and TFT (Imbrie and Kipp, 1971). During this study, two different

data bases were applied as reference data set for temperature estimations. Chapter 2 contains SST results derived from MAT that were obtained using the data base compiled by Pflaumann et al. (1996) which already included appropriate modern SSTs (Levitus and Boyer, 1994).

Data base "ATL916Lc-epo" (http://www.pangaea.de/Institutes/IfG/), originally compiled by Pflaumann and restricted to the northern hemisphere was used for both MAT and TFT (Chapter 3). Factors established by Principal Component Analysis and foraminiferal census data were calibrated to the modern SST for winter and summer based on values of 0-50 m water depth ($SST_{0\text{-}50m}$) which were extracted from the World Ocean Atlas (Levitus and Boyer, 1994) and linearly interpolated for the core top sites (Fig. 1.3).

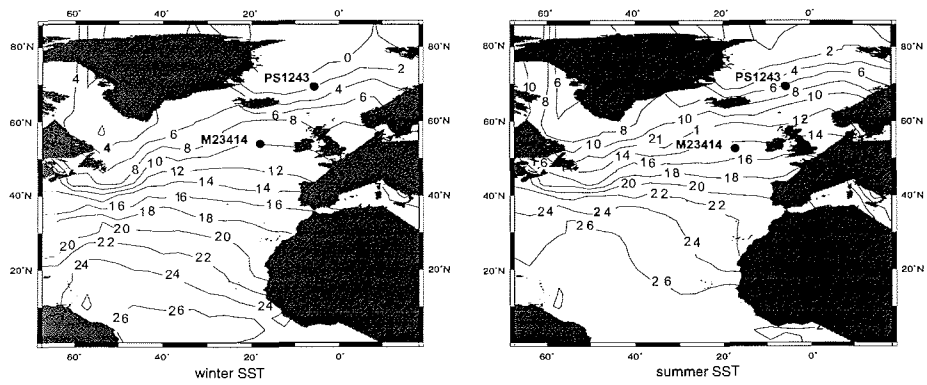

Fig. 1.3. Summer and winter sea surface temperature distribution (0-50m) according to Levitus and Boyer (1984). Locations of the investigated cores are marked. Temperatures are indicated in color with 2°C resolution.

The MAT procedure is based on direct comparison of foraminiferal census data of a given sample with foraminiferal census counts of samples from the reference data set by mean of dissimilarity coefficient calculations that results in selection of the best analogues. In this study ten of the best analogs were selected on the base of the least values of Squared Chord Distance (1.1), that is considered to be the optimal dissimilarity index (Overpeck et al., 1985). Additionally similarity coefficients were calculated (1.2). PaleoSSTs were estimated by a weighted average of measured SSTs that corresponded to the selected best analogs.

$$D_{ij} = \sum_{1}^{n} (\sqrt{P_{ik}} - \sqrt{P_{jk}})^2 \qquad (1.1)$$

$$S_{ij} = \sum_{1}^{n} \sqrt{P_{ik} * P_{jk}} \qquad (1.2)$$

where D_{ij} and S_{ij} in formulas (1) and (2) are coefficients of dissimilarity and similarity, respectively; P_{ik} nad P_{jk} are normalized relative abundances of the k^{th} species in the i^{th} analogue sample from the used modern data base and in the j^{th} subject sample, respectively; n is a number of selected species in the data matrixes, therefore, $1 \leq k \leq n$.

When dissimilarity and similarity coefficients are computed and the best selected analogs are defined, the required SST are calculated according to formula (3):

$$t = \frac{\sum_{1}^{n} (T_k \cdot S_k)}{\sum_{1}^{n} S_k} \qquad (1.3)$$

where t is required paleoSST; T_k is SST corresponding to k^{th} analogue sample; S_k is a coefficient of similarity of the k^{th} analogue sample ; n is a number of the best selected analogue samples; therefore, $1 \leq k \leq n$.

The TFT procedure consists of two steps (Imbrie and Kipp, 1971). At first, the whole foraminiferal diversity of a data base is subdivided into several associations (factors) by mean of Principal Component Analysis which results in two characteristic values: factor scores and factor loadings. Factor score values correspond to the contribution of each species in each factor. Whereas factor loading values correspond to the contribution of the individual factors in each sample. Loadings and scores > 0.4 are significant (Davis, 1986). This step was performed using the software package CABFAC (Klovan and Imbrie, 1971). After a matrix was established, all factors of the data base and their multiples were regressed against measured temperatures which resulted in a final

equation that has the following form:

$$T = a + b_1 \cdot f_1 + ... + b_7 \cdot f_7 + b_8 \cdot f_1 \cdot f_2 + ... + b_{28} \cdot f_6 \cdot f_7 + b_{29} \cdot f_1^2 + ... + b_{35} \cdot f_7^2 \quad (1.4)$$

Where T is a required SST; f is a factor loading; a is a constant; $b_1...b_{35}$ are the regression coefficients. A stepwise 2nd degree nonlinear analysis was performed with the STATVIEW software.

As it was indicated in this study on the comparison of results applied to the same data base, MAT provides *in situ* a better accuracy of the estimated temperatures than TFT (Table 1.2).

Table 1.2. Comparison of calibration results derived from MAT and TFT methods

	MAT		TFT	
Number of samples in modern data base	721		721	
	winter	summer	winter	summer
Correlation coefficient	0.992	0.991	0.986	0.982
R^2	0.985	0.982	0.972	0.964
Standard deviation of residuals	1.019	1.060	1.392	1.469

However, under no-analogue conditions that indicated when proportions of species in fossil assemblages differ from proportions of species in modern faunal associations, the TFT approach might be more useful. The results of MAT and TFT estimations are listed in the appendix (Table A.2, A.3).

1.5. Individual studies

This thesis compiles three manuscripts (Chapters 2-4) that have been either accepted, submitted or is in the state of submission to peer-reviewed scientific journals. A short overview of each study is given. The references of each chapter are combined together with the references of chapter 1 and listed together in Chapter 6.

Chapter 2:

Surface ocean properties in the Northeast Atlantic during the last 500,000 years: Evidence from foraminiferal census data and iceberg-rafted debris.

Results of detailed faunal analysis and sea surface temperatures, derived from changes in foraminiferal diversity using Modern Analogue Technique (MAT), as well as records of ice-rafted debris were analyzed to reconstruct the glacial-interglacial and millennial-scale climate variability in the North Atlantic during the last 500,000 years. The focus is on climatic differences between various interglaciations and millennial-scale variability. It is shown that intensity and frequency of SSTs closely correlate with IRD events and that both records also reflect the overall glacial-interglacial trends.

Chapter 3:

Sea surface temperature variability in the North Atlantic during the last two glacial-interglacial cycles: comparison of faunal, oxygen isotopic, and Mg/Ca-derived records.

A multiproxy investigation was performed to reconstruct the detailed climatic evolution of the last two glacial-interglacial cycles. The foraminiferal-derived SSTs, calculated with Transfer Function Technique (TFT) and Modern Analogue Technique (MAT) were compared with two sets of planktic oxygen isotope records based on the polar species *N. pachyderma* (s) and the temperate-to-subpolar species *G. bulloides*. The results were then compared with SSTs, calculated from Mg/Ca ratios in *G. bulloides*. Differences in climate evolution are recognized for the glacial periods. Millennial-scale temperature variabilities reveal diminished amplitudes during peak interglacial conditions whereas during both glacial and interstadial times the SST pattern seems rather pervasive.

Chapter 4:

Implications of planktic foraminiferal size fractions for the glacial-interglacial paleoceanography of the polar North Atlantic

Foraminiferal diversities from different mesh-size fractions are tested to improve paleoceanographic tools in the polar North Atlantic region. Faunal analysis was performed on records covering time intervals with different climatic conditions such as

marine oxygen isotope stage (MIS) 8 to 7 and are then compared with the last 30 ka. It is found that fluctuations in the relative abundance of small-sized specimens of *Turborotalita quinqueloba* sensitively reflect warm surface water incursions from the Atlantic during the times with reduced climate contrasts.

Surface ocean properties in the Northeast Atlantic during the last 500,000 years: Evidence from foraminiferal census data and iceberg-rafted debris

Abstract

Climate variability on glacial-interglacial and millennial timescales were investigated in the North Atlantic using foraminiferal diversities, sea surface temperature (SST) derived from foraminiferal census counts using modern analogue technique (MAT), and data of iceberg-rafted debris (IRD). In general, SSTs reveal diminished interglacial climate variability over the last 500 ka. Warmest conditions are found for marine isotope stage (MIS) 5.5 and MIS 11. SSTs during MIS 13 and the Holocene are about 2°C colder, followed by the various less warm interglacial peaks during MIS 7 and 9. However, enhanced dissimilarity coefficients provided by MAT implies that derived SSTs may significantly deviate from real values. In combinations with detailed faunal analyses temperatures obtained for MIS 7, for instance, appear to be largely overestimated.

IRD values are strongly reduced during all interglacial peaks but enhanced during colder periods. Depending on the particular climatic mode IRD events reveal striking differences in both frequency and intensity. Peak glacial periods are marked by lowest SSTs and highest IRD input. While the IRD pattern during MIS 6 resembles that of the last glacial cycles having intensive changes, the period of MIS 7-9 is characterized by less climate contrasts. In nearly all cases IRD events show good correlations with decreases in SST and in relative abundance of the polar species *Neogloboquadrina pachyderma* sinistral (s), implying that the type of changes in surface ocean properties as known from the last glacial-interglacial cycle is a persistent feature of the northern hemisphere Pleistocene climate.

2.1. Introduction

According to recent concepts, the North Atlantic is a sensitive region for climate change in the Quaternary due to meltwater released from drifting icebergs effecting the thermohaline circulation (e.g. Rahmstorf, 1995; Broecker, 1997; Ganopolski and Rahmstorf, 2001). On glacial-interglacial timescales, temperature fluctuations exhibit large amplitudes in this area and are therefore useful for detailed climatic investigations. Previously, similarity of the peak interglacial conditions during the late Pleistocene has been revealed for this region, suggesting that sea surface temperatures (SST) in the North Atlantic reached their warm extreme during all interglacial periods of the last 500 ka, despite some differences in insolation values (Ruddiman and McIntyre, 1976; Ruddiman et al., 1986a, b). For the last climate cycle, it was recently discovered that millennial-scale climate oscillations are superimposed on the major glacial-interglacial trend (Bond and Lotti, 1995; Elliot et al., 1998; van Kreveld, 2000). The most severe of these events are identified as prominent layers of iceberg-rafted debris (IRD), so-called Heinrich-events (Heinrich, 1988; Bond et al., 1992).

Meltwater released by icebergs during these Heinrich events apparently prevented northward-directed heat transfer by shutting down global thermohaline circulation (Broecker, 1994b; Sarnthein et al., 2001). Accordingly, drastic changes in sea surface temperature (SST) and salinity are associated with Heinrich-events (Bond et al., 1992; Maslin and Shackleton, 1995). They are known as persistent feature in the North Atlantic during the last 130 ka, punctuating glacial, interstadial, as well as interglacial intervals (e.g. McManus, 1994; Bond et al., 1997; Chapman and Shackleton, 1999). However, investigations of older time intervals are relatively sparse, but do indicate that short-term climatic oscillations also occurred in previous glacial and interglacial cycles (Oppo et al., 1998; McManus, 1999; Didié and Bauch, 2000).

In the present investigation, our objective is to study the climate of the last 500 ka in order to trace principal features of climate oscillations throughout various climatic modes by directly comparing surface ocean proxy records of IRD, planktic foraminiferal diversities, SST estimates and relative abundance of the polar foraminifera *Neogloboquadrina pachyderma* sinistral (s).

2.2. Material and methods

Marine sediment core M23414 (53°32´N, 20°17´W, water depth 2200 m; Helmke and Bauch, 2001) has been recovered from a site situated under the North Atlantic Drift (Fig. 2.1), within the IRD belt (e.g. Ruddiman, 1977; Grousset et al., 1993). Therefore, this location is well-suited to study changes in surface ocean properties as it is affected by both iceberg drift during cold periods and warm water advection during warm time intervals. The stratigraphic subdivision of M23414 is based on a centimeter-sampled lightness record aligned to SPECMAP chronology and reaches back to marine isotope stage (MIS) 13 (Helmke and Bauch, 2001, Helmke et al., 2002). The chronology of the uppermost section of M23414 is supported by AMS ^{14}C age-measurements (Didié et al., 2002) and by assignment of the well-known ages of Heinrich events 1-6 to our core (Fig. 2.2).

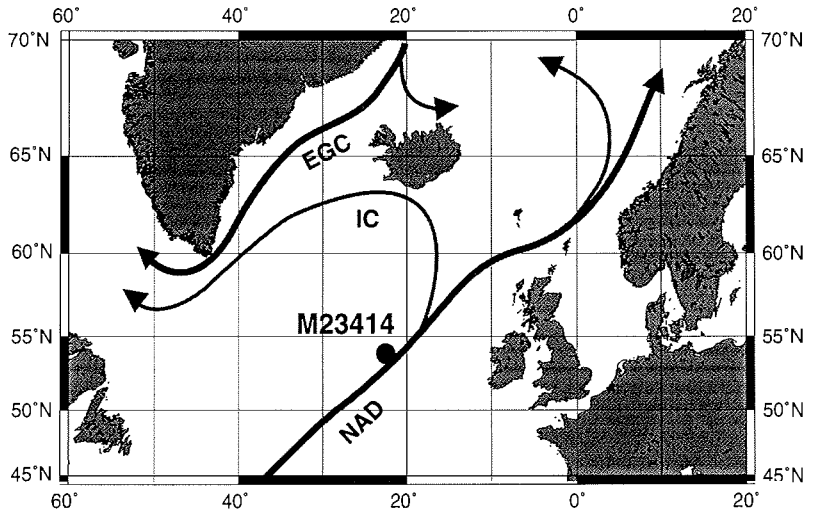

Fig. 2.1. Core location and general modern surface circulation pattern in the investigated area; NAD – North Atlantic Drift, EGC – East Greenland Current, IR – Irminger Current.

Sediment residues were derived from 1 cm thick slab samples. IRD were counted in the >250 µm size fraction at 2.5 cm depth intervals. Faunal counts were executed in 5 cm steps using two size fractions >150 µm; a minimum of 300 specimens was counted per sample. The modern analogue technique (MAT) of Prell (1985) using a reference

of 738 core top samples (Pflaumann, 1996) and oceanographic sea surface temperature data (Levitus and Boyer, 1994) was applied to estimate past SSTs. The 10 best analogues (lowest dissimilarity) for every core sample were chosen for final SST calculations. The Squared Chord Distance was used as index to determine the dissimilarity coefficient (Overpeck et al., 1985).

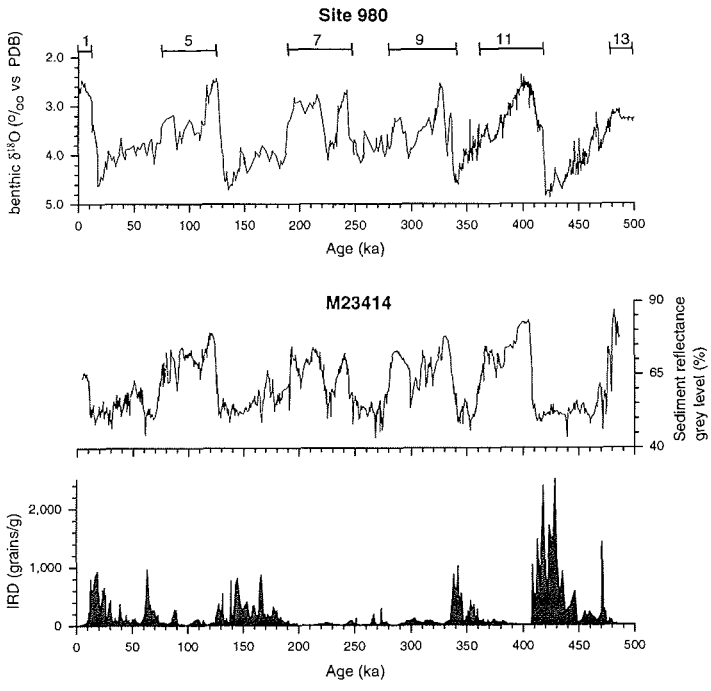

Fig. 2.2. Stratigraphic subdivision of core M23414 showing records of sediment lightness (L*) and IRD >250 μm expressed as grains per gram of dry sediment (from Helmke et al., 2002) in comparison with benthic $\delta^{18}O$ of *Cibicidoides wuellerstorfi* from nearby ODP site 980 (55°29´N, 14°42´W; from McManus et al., 1999); marine isotope stage boundaries as indicated.

2.3. Glacial-interglacial variability

2.3.1. Sea Surface Temperatures

The seasonal SST records deduced from the foraminiferal census counts show high-swing glacial-interglacial oscillations (Fig. 2.3). Interglacial SSTs varied between 8 and 16°C and between 4 and 12°C for summer and winter respectively. Glacial phases are

marked by considerably colder SSTs, reaching minimum values of 4°C during warm seasons and 1°C during cold seasons. During major climate transitions SSTs underwent large shifts of 8-10°C.

Peak interglacial maxima are marked by comparable summer temperature of about14°C. The only exception is MIS 5.5 that appears as the warmest interglacial extreme with summer temperatures of 16°C. This is on average 2°C warmer than the present temperatures in this region. Low peak interglacial climate variability in M23414 is in accordance with previous investigation in the North Atlantic (Ruddiman and McIntyre, 1976; Ruddiman et al., 1986a, b). However, not taking into account the differences in insolation values, quite contrasting oceanographic regimes between the North Atlantic and the adjacent Nordic seas can be inferred for peak interglacials such as MIS 5.5 and 11 (e.g., Bauch et al., 1999; Bauch et al., 2000a, b). Interesting in this respect is also MIS 7, which in the Nordic seas, appears as a rather cold interval (Kandiano and Bauch, in press).

In core M23414, MIS 7 exhibits its typical three warm peaks in the substages. Although SSTs were nearly as warm as in the Holocene or MIS 9, MIS 7 has the highest dissimilarity coefficients (Fig. 2.3); even for the first best analogues they already exceed a value of 0.1. This strongly indicates a no-analogue situation during MIS 7, implying that estimated temperatures may deviate considerably from the actual values. The Imbrie and Kipp (1971) technique, as employed by Ruddiman et al. (1986a b), does not provide a sensitive index of a no-analogue situation (Mekik and Loubere, 1999). Hence, SSTs for MIS 7 obtained by us as well as by previous researchers appear to be overestimated. That the overall climatic conditions in MIS 7 were colder than during other peak interglacials is indirectly corroborated also by comparatively high benthic $\delta^{18}O$ values recorded in nearby the ODP core (Fig. 2.2).

On the basis of SSTs record and the dissimilarity index, only MIS 11 seems to match as close analogue to the Holocene. This gains supports from other regions where similar climatic conditions are observed for these two periods (e.g., Howard, 1997). However, it should be mentioned that multiproxy investigations in the Nordic seas have revealed striking differences between MIS 1 and MIS 11. These do indicate a much weaker advection of warm Atlantic surface water masses into the Nordic seas during MIS 11

than in the Holocene (Bauch et al., 2000b), implying a steeper SST gradient between the polar and subpolar North Atlantic for MIS 11.

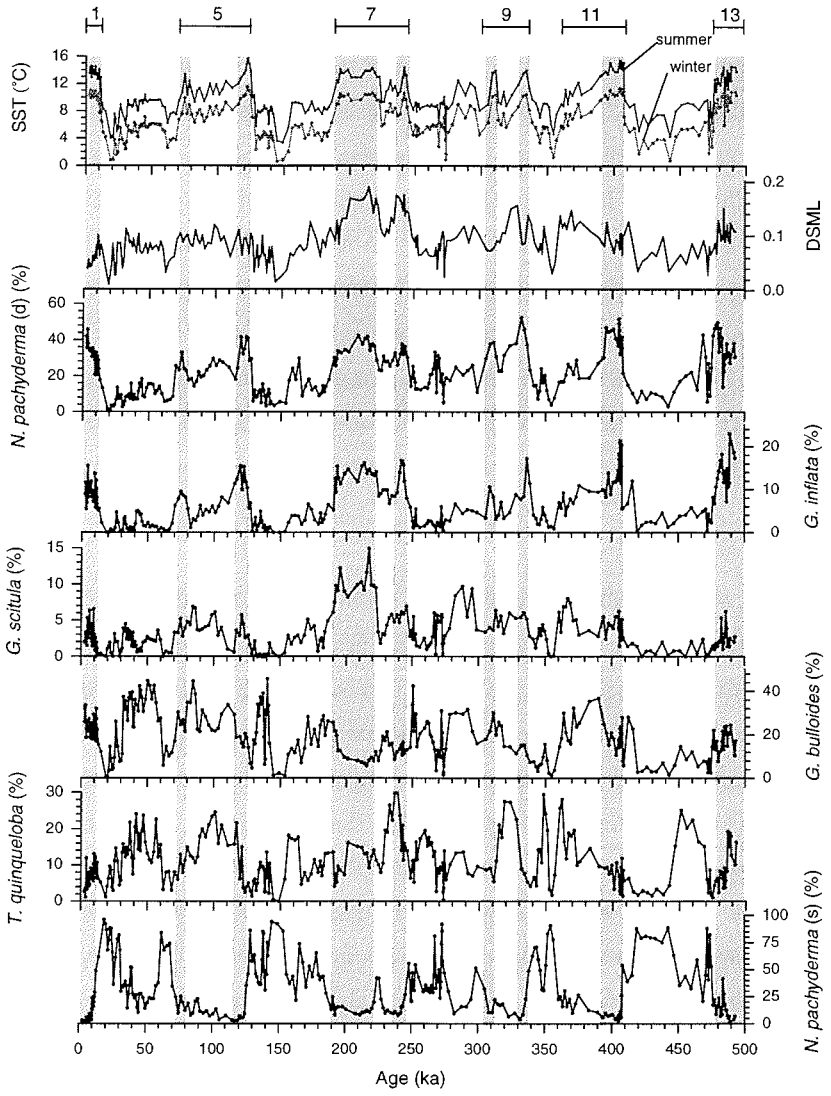

Fig. 2.3. Relative abundance of dominant planktic foraminifers alongside with MAT-derived SSTs and a dissimilarity coefficient (DSML) based upon the 10 best analogues; shaded areas indicate climatic maxima as recognized on the basis of SST estimates.

2.3.2. Planktic foraminiferal composition related to a no-analogue situation

Although a number of recent studies were focused on estimating past SSTs for North Atlantic glacial-interglacial cycles, comparatively little is published in detail about

species other than the polar species *N. pachyderma* (s). A closer look at the foraminiferal assemblages based on the best analogue fauna from MIS 7 with high dissimilarity index reveals some interesting features (Fig.2.3). Along with relatively high number of species that are abundant in the temperate climatic zone, e.g. *N. pachyderma* (d), *Globorotalia inflata*, and *Globorotalia scitula*, the subpolar foraminifera *Turborotalita quinqueloba* yields its maximum of 30 %, and *N. pachyderma* (s) reaches values of 12-16%. This high value in the latter is twice as much as during peak interglacials MIS 1, 5.5 and 11, thus indicating comparatively lower temperatures. On the other hand, the abundance of *Globigerina bulloides* is on average twice as much lower than in the reference best analogue samples.

The no-analogue situation found in MIS 7 may be caused by complex environmental circumstances, for which temperature is important but by no means the sole factor that controls foraminiferal species abundance. For instance, it was found by Loubere (1981) that *G. inflata* shows a strong relationship to seasonality, becoming more abundant as annual thermal contrast increases; the distribution of *G. bulloides* seems strongly related to the particular upper ocean density structure and/or to phytoplankton productivity. Therefore, a combination of several environmental factors could lead to a foraminiferal assemblage not observed in the reference core top samples.

On the other hand, a simultaneous occurrence of subpolar and temperate planktic foraminiferal species, of which the watermass relationship is relatively well known, may allow us to make detailed assumptions about past oceanographic situation. For *T. quinqueloba*, a close association with polar water mass fronts is inferred from core top sediments of the North Atlantic and the Nordic seas (Barash, 1988; Johannessen, 1994). Thus, the high values of *T. quinqueloba* during MIS 7 in core M23414 may indicate proximity of polar waters to this site, whereas an increased abundance of temperate water species is more characteristic for a direct influence of relatively warm Atlantic water masses.

2.4. Millennial-scale climate variability

Quasi-periodically occurring IRD events associated with a decrease in SST are recognized by us for both glacial and interglacial time intervals. IRD is extremely

diminished during interglacial peaks but usually enhanced during glacial periods, reaching its maximum during MIS 12 (Fig. 2.2, 2.4a). This is in accordance with studies from other regions that consider MIS 12 to be a particularly severe glaciation (Howard, 1997; Rohling et al., 1998; Bauch and Erlenkeuser, in press). In general, maxima in IRD deposition are also coincident with increased global ice volume, as documented by benthic $\delta^{18}O$ (Fig. 2.2), implying that the global ice volume appears to be an important factor that controls the occurrence of IRD in the Northeast Atlantic (McManus et al., 1999).

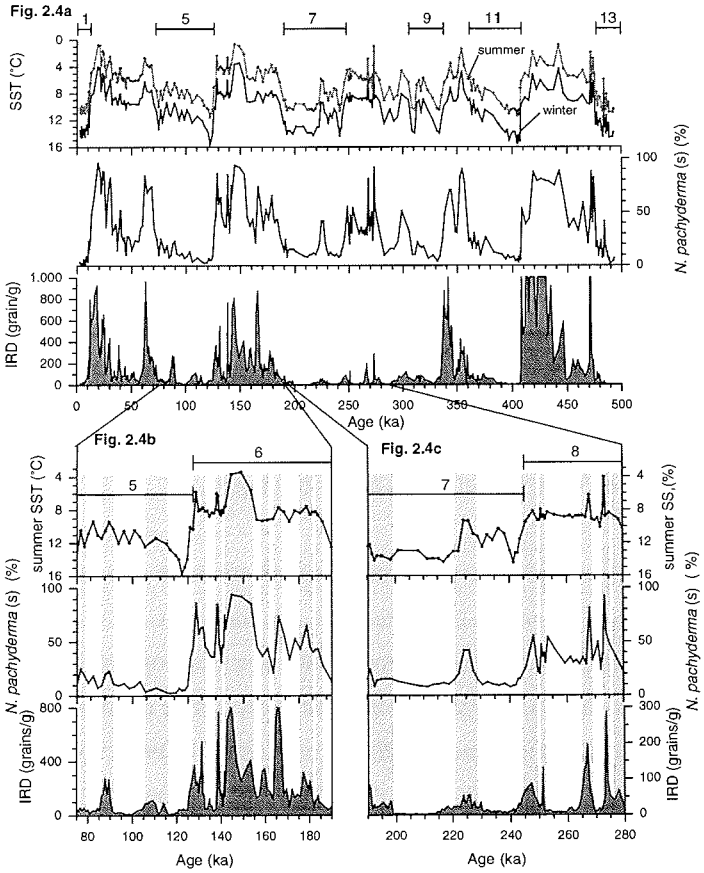

Fig. 2.4. Record of IRD in comparison with SSTs (reversed axis) and relative abundance of *N. pachyderma* (s); note that the maximum IRD amount in MIS 12 is cut off to emphasize low-amplitude fluctuations (Figure 2.4a). Insets below are shown for a detailed description of MIS 6-5 with pronounced glacial-interglacial fluctuations (Figure 2.4b) and the diminished climate contrasts which characterize MIS 8-7 (Figure 2.4c); shaded areas indicate cold events with a corresponding response in all three proxies.

Comparison of two climate cycles with contrasting surface water conditions, MIS 6-5 and MIS 8-7, show striking differences in both intensity and frequency of IRD events and surface water cooling (Fig. 2.4b, 2.4c). The high-frequency climate variability observed in MIS 6 resembles the classical features known from the last glacial cycle (~60-15 ka). In contrast, the MIS 8-7 period is marked by only few cold events. The low number of events as well as the maximum IRD values of only up to 300 grains make this time interval similar to the younger part of MIS 5 (~115-75 ka).

Despite differences in frequency and intensity, most IRD events correlate with corresponding excursions in the *N. pachyderma* (s) record. This means that principal characteristics of so-called Heinrich events can be recognized in the Northeast Atlantic for most of the last 500 ka, implying that the dynamics of circum-North-Atlantic ice sheets and its influence on the thermohaline circulation via controlling surface ocean salinity and temperature is a persistent feature of the northern hemisphere climate. However, to more precisely quantify surface ocean properties based on foraminiferal census data, it is conceivable that new approaches of modified TFTs are in need (e.g., Mix et al., 1999) in order to circumvent no-analogue problems.

2. 5 Conclusions

Planktic foraminiferal relative abundances, SSTs derived from the MAT method, and IRD records were carefully examined in the North Atlantic core for the last five glacial-interglacial cycles. It was found that MIS 5.5 exhibits the warmest climatic conditions whereas SSTs for the other peak interglacial interval were as much as 2°C colder. However, SSTs for MIS 7 seem to be overestimated, which is inferred from enhanced dissimilarity coefficients provided by MAT. This, in turn, is caused by an unusually high abundance of subpolar species registered during MIS 7.

Millennial-scale sea surface changes are recognized during the entire investigated interval. The amplitude of short-lived SST oscillations is strongly reduced during peak interglacial conditions and enhanced during glaciations and interstadials. It was also found that IRD deposition, related to millennial-scale climate fluctuations, change in both frequency and intensity depending on the particular climate mode. These IRD events are more pronounced during severe glacial periods.

Sea surface temperature variability in the North Atlantic during the last two glacial-interglacial cycles: comparison of faunal, oxygen isotopic, and Mg/Ca-derived records

Abstract

Sea surface temperatures (SST) were reconstructed from a core site in the North Atlantic using planktic foraminiferal census counts and Mg/Ca measurements. The faunal SSTs are derived from transfer function and modern analogue techniques. The results were compared with oxygen isotope records obtained from two planktic foraminifera species, *Neogloboquadrina pachyderma* sinistral (s) and *Globigerina bulloides*, and records of iceberg-rafted debris (IRD). In general, temperature estimates indicate slightly warmer climatic conditions during marine oxygen isotope (MIS) 5.5, the marine analogue of the Eemian, than during the Holocene. Differences in climatic development are recognized for the glacial periods. In contrast to the last glaciation when the temperature minimum is coincident with the maximum in global ice volume, the temperature minimum of the penultimate glaciation preceded the maximum in global ice volume.

Millennial-scale temperature variabilities reveal diminished amplitudes during peak interglacial conditions but over glacial and interstadial times the pattern seems rather consistent. Slight initial cooling episodes that preclude the main IRD event were registered in all cases. The IRD events are coincident with abrupt SST decrease of 3-5°C.

Mg/Ca-derived SSTs clearly mimic the overall glacial-interglacial trend, however, they reveal considerable offsets from faunal-derived records due to deficiency in calibration of the latter method and/or existence of additional factors controlling Mg uptake in *G. bulloides* tests.

3.1. Introduction

Since the first quantitative sea surface temperature (SST) estimates, based on alterations in faunal diversity from North Atlantic sediments revealed the main glacial-interglacial pattern of the late Quaternary (Ruddiman and McIntyre, 1976, 1984; Ruddiman et al., 1986a, b), a great bulk of new information was obtained which improved our present knowledge of climate change during this period. It was discovered that abrupt short-lived climate events punctuate both glacial and interglacial periods. In Greenland ice cores they were recognized as Dansgaard-Oeschger cycles (e.g. Johnsen et al., 1992; Dangaard et al., 1993; Grootes et al., 1993; Grootes and Stuiver, 1997), of which each cycle starts with a short warm event and terminates in a considerable cooling. The most severe of these cooling episodes are associated with circum-North-Atlantic ice sheet collapses and are identified in North Atlantic marine sediment records by enhanced deposition of iceberg-rafted debris (IRD), material delivered from melting iceberg flotillas, and a decrease in planktic $\delta^{18}O$ caused by input of meltwater (Heinrich, 1988; Bond et al., 1992; Bond et al., 1993; Bond and Lotti, 1995). Moreover, these millennial-scale climate fluctuations seem to be a global feature being registered also off northwest Africa (Zhao et al., 1995), in the Carribean Sea (Hüls and Zahn, 2000), in the North Pacific (Kotilainen and Schakleton, 1995), in the South China Sea (Wang et al., 1999) and in Antarctic ice cores (Blunier et al., 1998).

According to recent concepts, variations in thermohaline circulation are regarded as the main mechanism that may amplify an initial impulse thereby changing climate to different modes (Oppo and Lehmann, 1995). In turn, changes in thermohaline circulation occur when sea surface properties (e.g. salinity, temperature) for any current mode are distorted (Seidov and Maslin, 1999; Marotzke, 2000; Ganopolski and Rahmstorf, 2001; Clark et al., 2002). Therefore, detailed investigations of sea surface property changes are extremely important to understand climate driving mechanisms. In this respect sea surface temperature (SST) reconstructions appear to be the most useful aspect that also helps to conduct modeling experiments and, therefore, future climate prediction. The usefulness of multiproxy approaches to paleotemperature estimations were broadly discussed by previous researchers (Bard, 2001; Nürnberg et al., 2000; Lee and Slowey, 2001). Due to definitive shortcomings of the well-established SST methods

every new independent approach that can translate a paleotemperature signal is of great interest for paleoceanographers.

Here we present high resolution paleotemperature records for the last two glacial-interglacial cycles inferred from foraminiferal census counts calculated with modern analogue (MAT) (Prell, 1985) and with transfer function techniques (TFT) (Imbrie and Kipp, 1971). Results of these traditional approaches of SST estimations based on changes in faunal diversity are compared with temperatures derived from Mg/Ca measurements, performed on *Globigerina bulloides*. This method was recently reintroduced as a useful paleoceanographical tool after researchers had found that temperatures are an important factor controlling the chemical composition of foraminiferal tests (e.g. Puechmaille, 1994; Nürnberg et al., 1996; Nürnberg et al, 2000). SST results are supported by $\delta^{18}O$ measurements performed on two planktic foraminiferal species, *N. pachyderma* sinistral (s) and *G. bulloides* and IRD records with emphasis on comparing climate conditions during glacial periods and how they relate to millennial-scale variability.

3.2. Material and methods

3.2.1. Oceanographic setting, core location, and stratigraphy

The hydrography of the North Atlantic region is mainly determined by input of high saline relatively warm waters brought northward into the Nordic seas by the North Atlantic Drift (NAD). The counterpart of this northward-flowing warm current is the East Greenland Current (EGS) that transports cold water from Arctic Ocean southward along the eastern coast of Greenland. During warm periods like today these high-saline Atlantic surface waters gain high density due to cooling in the polar latitude and sink to the abyss promoting global ocean conveyor (Broecker and Denton, 1990). During glacial periods Atlantic waters could not penetrate so far north, partly due to the widespread occurrence of polar waters.

Gravity core M23414-9 (53.537 °N; 20.288 °W; water depth 2199), spliced together with trigger-box core M23414-6 (53.537 °N; 20.537 °W; water depth 2201), was selected for the study. This core is situated under the NAD (Fig. 3.1) and within the

glacial IRD belt (Ruddiman, 1977; Grousset et al., 1993). Therefore, millennial-scale oscillations can be traced at this location quite successfully, not only by records bearing temperature signals, but also by changes in IRD deposition (Helmke et al., 2002). The selected core is situated well above the lysocline during glacial as well as interglacial times and the foraminiferal taphocenoses were not affected by significant carbonate dissolution.

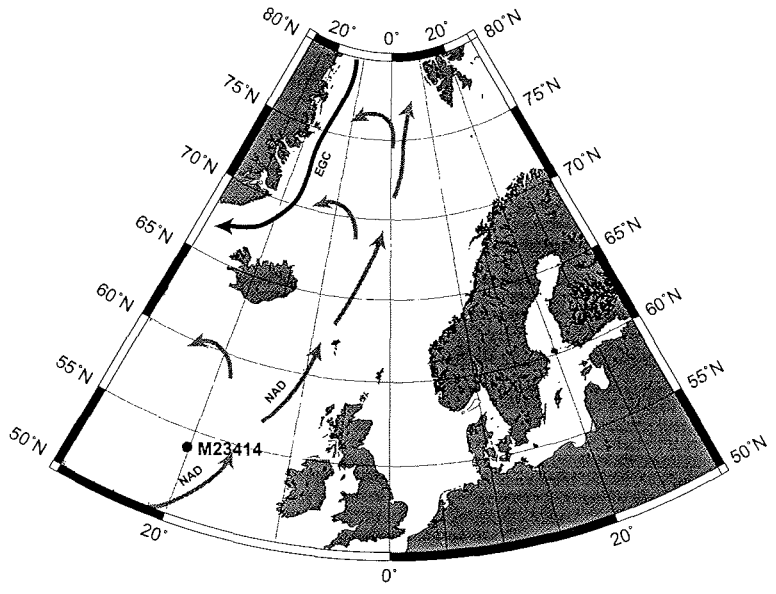

Fig. 3.1. Geographical position of the investigated core site and generalized oceanographic circulation. NAD – North Atlantic Drift, EGC – East Greenland Current, IR – Irminger Current.

The stratigraphic subdivision of M23414 is based on planktic oxygen isotope records and in addition on a centimeter-sampled lightness record aligned to SPECMAP chronology (see for details Helmke and Bauch, 2001, Helmke et al., 2002). The investigated section of the core reaches back to MIS 7 (Fig. 3.2). The chronology of the uppermost section of M23414 is also supported by AMS ^{14}C age-measurements and by assignment of the well-known ages of Heinrich events (H) 1-6 to our core (Didié et al., 2002).

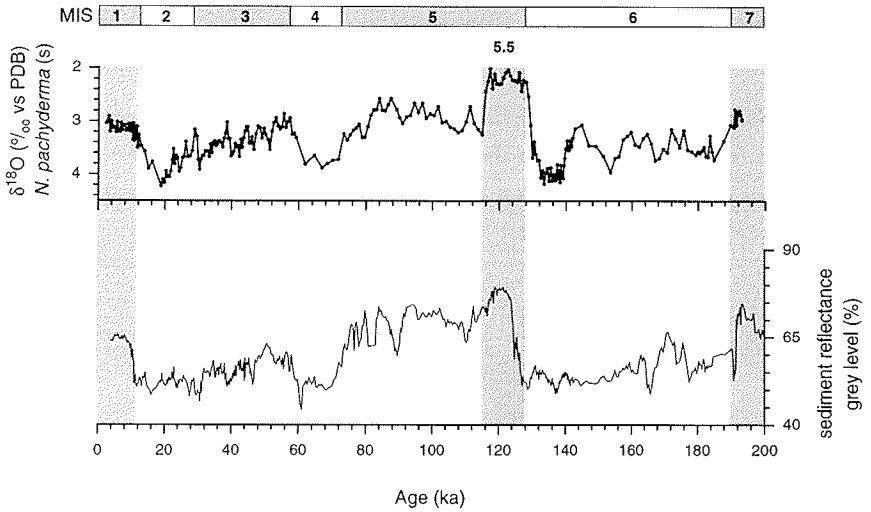

Fig. 3.2. Stratigraphic subdivision of core M23414 established on the base of sediment lightness. Marine isotope stages (MIS) are indicated. Gray bars show peak interglacial conditions.

3.2.2. Faunal-derived SST

3.2.2.1. Sample processing

Foraminiferal analyses were performed in 2.5 cm steps. Samples have been taken as 1 cm slabs and processed through freeze-drying, washing and sieving over 150 µm mesh-size to obtain consistency with the modern foraminiferal data base. To better facilitate the counting procedure, each sample was sieved into two subfractions: 150-250 µm and >250 µm. Then each subfraction was split down to 150-300 specimens and counted. Relative abundances for the entire sample were then recalculated using the appropriate split factor. Foraminiferal abundances were examined following the taxonomic concepts of Bé (1977), Kennett and Srinivasan (1983), Saito et al. (1981) and Hemleben et al. (1989).

3.2.2.2. Data base and species selection

A new enlarged database of the Atlantic ocean, consisting of 916 samples and compiled by U. Pflaumann ("ATL916Lc-epo" http://www.pangaea.de/Institutes/IfG/), was taken for the SST estimations based on foraminiferal census counts. We restricted the database to the northern hemisphere only (0.3 °N to 86.41 °N), since foraminiferal distribution patterns show slightly different temperature responses in the northern and southern hemispheres due to differences in water mass circulation (Barash, 1988;

Niebler and Gersonde, 1998). It was also shown by Le and Shackleton (1994) that regional calibrations achieve better accuracy than global data sets. A total of 721 core-top samples were therefore considered as reference data base for this study. Foraminiferal census data and the factors derived from TFT procedure were calibrated to the modern winter and summer SST based on values from 0-50 m ($SST_{0\text{-}50m}$) water depth. These oceanographic data were extracted from the World Ocean Atlas (Levitus and Boyer, 1994). The used winter and summer temperatures represent average values for February-April and August-October respectively.

Finally, 29 species (Table 3.1) were selected for both MAT and TFT quantitative analyses following in general the strategy of Pflaumann et al. (1996). Intergrades between *Neogloboquadrina pachyderma* dextral (d) and *Neogloboquadrina dutertrei* were grouped together to avoid taxonomic controversies with previous investigations. Left and right coiling varieties of *Globorotalia truncatulinoides* were considered separately. According to previous investigations, these two varieties posses different genotypes (de Vargas, 2001) and show different, temperature-dependent geographical distribution (Herman, 1972; Barash, 1988).

3.2.2.3. TFT procedure

The TFT procedure was executed in two steps. At first, Q-mode Principal Component Analysis (PCA) combined a large number of species into a smaller number of factors that describe foraminiferal associations. This was performed with the Fortran software package CABFAC and THREAD (Klovan and Imbrie, 1971). In a second step, all defined factor loadings were regressed against modern SSTs and the obtained equation was applied to down core records using the StatView program.

The first step procedure results in seven factors. Factor scores of each species are shown in Table 3.1. The geographical distribution of these seven factors generally resembles those of earlier factor models (Imbrie and Kipp, 1971; Kipp, 1976; Molfino, et al., 1982; Dowsett and Poore, 1990; Hüls and Zahn, 2000) (Fig. 3.3). Values of factor loadings that are lower than 0.4 can be considered unimportant for the analysis (Davis, 1986).

Table 3.1. Varimax factor score matrix.

Spesies	Factor 1	Factor 2	Factor 3	Factor 4	Factor 5	Factor 6	Factor 7
Globigerinella aequilateralis	-0.002	0.001	0.091	0.008	0.054	-0.021	-0.017
Globigerina bulloides	0.213	0.003	-0.032	**0.937**	0.016	-0.147	-0.148
Globigerina calida	0.005	-0.001	0.015	0.001	0.000	0.018	0.007
Globorotalia conglobatus	-0.002	0.000	0.019	0.000	0.000	0.014	0.000
Globorotalia crassaformis	-0.002	0.001	0.013	-0.003	0.057	0.006	0.002
Sphaeroidinella dehiscens	-0.001	0.000	0.002	-0.002	0.019	0.001	0.003
Beella digitata	0.001	0.000	0.005	0.003	0.015	0.000	-0.004
Neogloboquadrina dutertrei	0.000	0.004	0.022	0.037	**0.628**	0.022	-0.025
Globigerina falconensis	-0.003	-0.002	0.044	0.036	-0.073	0.145	0.034
Globigerinita glutinata	0.142	-0.026	0.142	0.180	-0.057	0.010	**0.493**
Globorotalia hirsuta	-0.007	0.000	0.011	0.043	-0.026	0.057	-0.014
Turborotalita humulis	0.000	-0.001	0.013	0.006	-0.020	0.032	0.000
Globorotalia inflata	0.110	-0.009	0.027	0.107	0.134	**0.930**	-0.003
Candeina nitida	0.000	0.000	0.002	0.000	0.000	-0.001	0.000
Pulleniatina obliquiloculata	-0.003	0.001	0.023	-0.007	0.110	-0.014	0.008
Neogloboquadrina pachyderma (s)	-0.035	**0.993**	-0.003	0.008	-0.012	0.020	-0.077
Neogloboquadrina pachyderma (d)	**0.957**	0.036	0.023	-0.250	-0.006	-0.075	-0.085
Turborotalita quinqueloba	0.047	0.111	-0.011	0.043	0.028	-0.049	**0.841**
Globigerinoides ruber (r)	-0.004	0.002	0.094	-0.008	0.084	-0.056	0.004
Globigerinoides ruber (w)	-0.034	0.005	**0.912**	0.011	**-0.225**	0.041	-0.054
Globigerina rubescens	0.003	-0.001	0.026	0.013	-0.020	0.011	-0.008
Globigerinoides sacculifer trilobus	-0.016	0.007	**0.308**	-0.001	0.390	-0.217	-0.068
Globigerinoides sacculifer sacculifer	-0.003	0.002	0.131	-0.030	0.151	-0.077	0.018
Globorotalia scitula	0.018	-0.004	0.011	0.045	-0.011	0.034	0.000
Globigerinoides tenellus	-0.001	0.000	0.025	0.003	-0.018	0.001	0.002
Globorotlia truncatulinoides (s)	-0.008	0.000	0.039	0.023	-0.056	0.109	0.009
Globorotlia truncatulinoides (d)	0.002	-0.002	0.034	0.044	-0.027	0.083	-0.028
Orbulina universa	0.021	-0.001	0.028	-0.004	0.038	0.026	-0.023
Globorotalia menardii-tumida group	-0.014	0.007	0.084	-0.050	0.565	-0.003	0.063

High factors scores of characteristic species that define factors are indicated in bold numbers

The first three factors are closely related to climatic zones and are defined by a strong temperature dependence (Fig. 3.4). Factor 1 represents the temperate assemblage, dominated by *N. pachyderma* (d); Factor 2 is strongly dominated by *N. pachyderma* sinistral (s) and reflects polar conditions; Factor 3 corresponds to the tropical assemblage with high factor score of the white variety of *Globigerinoides ruber* (w).

Factor 4, represented by *G. bulloides*, is superimposed on Factor 1 and may be considered as a subgroup of this factor. This factor distribution also shows a temperature dependence, although it is apparently complicated by influence of other environmental components (Fig. 3.4). This species, being adopted to a wide temperature range (Be and Tolderlund, 1971; Barash, 1988), also characterizes upwelling situations regardless of their geographical position (Ganssen and Sarnthein, 1983), and seems sensitive to high-fertility conditions (Vincent and Berger, 1981). These four factors

make the main contribution and describe 68.5% of the variance whereas the remaining 7.5% of variance are described by the other three factors (Table 3.2).

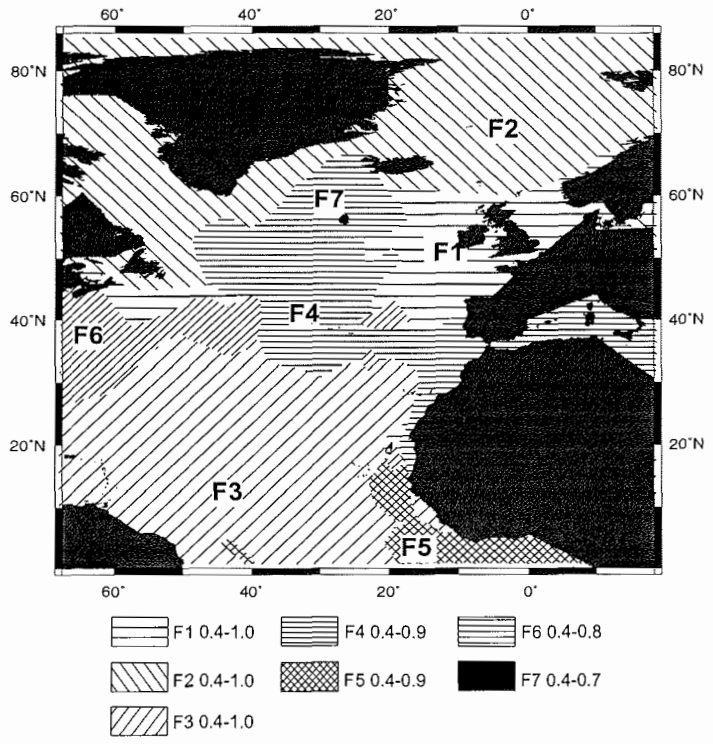

Fig. 3.3. Generalized geographical distribution of factors resulted from Principal Component Analysis of 721 core tops. Factor loadings are indicated by colors. Core locations are shown as dots.

Table 3.2. Statistics of PCA

	factor 1	factor 2	factor 3	factor 4	factor 5	factor 6	factor 7
Variance (%)	42.30	23.19	16.99	6.02	3.28	2.83	1.39
Cumulative variance (%)	42.30	65.49	82.48	88.50	91.77	94.60	96.00

For the remaining three factors temperature not solely controls the faunal association (Fig 3.4). Factor 5 is restricted to the western coast of Africa and is characterized by a high factor score of *N. dutertrei*, a species which is common in tropical upwelling environments (Kipp, 1976, Parker and Berger, 1971; Prell and Curry, 1981). For this factor a negative value of the factor score is also characteristic for *G. ruber* (w) which indicates that lowered temperatures are typical for this area.

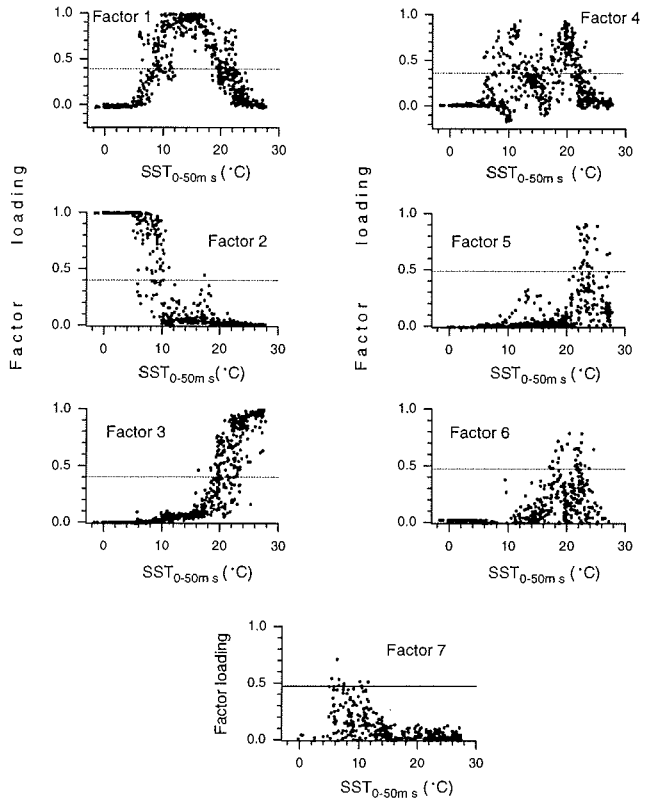

Fig. 3.4. Summer SST dependence of the factors represented by different foraminiferal assemblages. SST are given for the 0-50 m water depth. Dashed lines indicate factor loading significance (>0.4).

The geographical distribution of Factor 6 is coincident with deep ocean areas where carbonate sediments are affected by dissolution. In such regions, the abundances of species with thickened shells are preferentially increased (Berger, 1968, Barash, 1988). This factor is therefore mainly described by relative abundance of *Globorotalia inflata* that reaches 40-48% in abyssal regions and in the Newfoundland depression where the depth of the see bottom is well below the lysocline. Although Factor 6 is primarily controlled by preferential dissolution it also shows a temperature dependence (Fig 3.4).

Factor 7 is characterized first of all by an elevated factor score of *Turborotalita quinqueloba*, whose abundance significantly increases at the oceanographic fronts, as it was already shown by Carstens et al. (1997) for the Nordic seas region. In fact, the

relative abundance maximum of this species is found at the edge of the North Atlantic Current where it reaches nearly 49% in the modern database. This factor, as well as Factor 4, represents a subgroup of Factor 1 (Fig 3.4).

Table 3.3. Correlation coefficients for TFT regression analysis of winter $SST_{0\text{-}50m}$

	Coefficient	Standard Error	Standard Coefficient	F to remove
Intercept	12.719	0.557	12.719	521.471
F1	-4.656	0.544	-0.205	73.191
F2	-11.889	0.592	-0.573	403.013
F3	12.555	0.583	0.542	464.037
F5	10.840	1.014	0.239	114.331
F1F2	21.006	2.592	0.280	65.705
F1F4	11.714	1.717	0.212	46.533
F1F5	-13.966	2.459	-0.076	32.254
F1F6	7.483	0.817	0.083	83.914
F1F7	-9.309	1.435	-0.070	42.061
F2F4	-7.968	1.576	-0.049	25.573
F2F7	2.932	0.946	0.025	9.614
F3F4	-8.142	0.789	-0.110	106.379
F3F5	-6.504	1.453	-0.083	20.027
F3F6	-6.527	0.821	-0.71	63.281
F3F7	12.447	2.631	0.034	22.376
F4F5	6.913	2.622	0.031	6.954
F4F7	-15.351	1.552	-0.107	97.821
F1^2	-21.874	5.582	-0.115	15.356
F3^2	-18.540	3.767	-0.122	24.223

The communalities of the developed factor model are never below 0.7, the mean value of communalities being 0.97 (Fig. 3.5). All samples with communalities lower than 0.9 are found in deep water areas from low latitudes where the foraminiferal assemblages are affected by selective dissolution and at the west coast of Africa where the temperature dependence of foraminifers is complicated by upwelling conditions. Established factors were related to the modern SSTs using a stepwise second-degree non-linear regression analysis (Table 3.3 and 3.4), the calibration between measured and estimated temperatures yields a high statistical robustness for the new developed TFT (Fig. 3.6a). A slight increase of the standard deviations in comparison to FA20 (Molfino et al., 1982) is due to the larger data base used by us.

Table 3.4. Correlation coefficients for TFT regression analysis of summer $SST_{0\text{-}50m}$

	Coefficient	Standard Error	Standard Coefficient	F to remove
Intercept	12.719	0.557	12.719	521.471
F1	-4.656	0.544	-0.205	73.191
F2	-11.889	0.592	-0.573	403.013
F3	12.555	0.583	0.542	464.037
F5	10.840	1.014	0.239	114.331
F1F2	21.006	2.592	0.280	65.705
F1F4	11.714	1.717	0.212	46.533
F1F5	-13.966	2.459	-0.076	32.254
F1F6	7.483	0.817	0.083	83.914
F1F7	-9.309	1.435	-0.070	42.061
F2F4	-7.968	1.576	-0.049	25.573
F2F7	2.932	0.946	0.025	9.614
F3F4	-8.142	0.789	-0.110	106.379
F3F5	-6.504	1.453	-0.083	20.027
F3F6	-6.527	0.821	-0.71	63.281
F3F7	12.447	2.631	0.034	22.376
F4F5	6.913	2.622	0.031	6.954
F4F7	-15.351	1.552	-0.107	97.821
F1^2	-21.874	5.582	-0.115	15.356
F3^2	-18.540	3.767	-0.122	24.223

3.2.2.4. MAT procedure

MAT procedure is based on a direct comparison of faunal diversities in a given sample with faunal diversities of the reference data set which results in selection of samples, so-called best analogues with the most similar faunal composition. The ten best analogues have been chosen on the base of the squared chord distance dissimilarity index (Overpeck et al., 1985). PaleoSSTs were estimated by a weighted similarity SST average of the chosen best analogues. The statistical robustness of the MAT based on the enlarged data set (Fig. 3.6b) is very close to MAT results produced by other researchers that have used lesser reference data samples in the North Atlantic region (Waelbroeck et al., 1998; Hüls and Zahn, 2000).

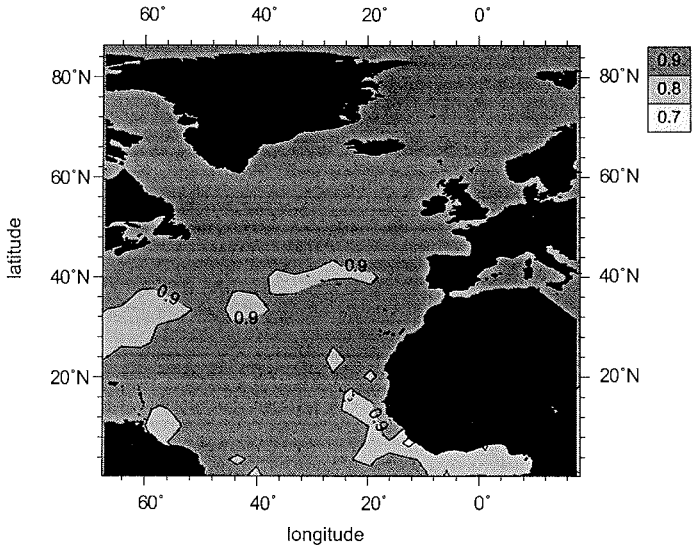

Fig. 3.5. Geographical distribution of the communalities derived from the factor model based on the 721 core topes.

3.2.3. Mg/Ca SST estimation

3.2.3.1. Sample processing and calibration

Mg/Ca measurements have been performed in 10 cm steps using the same samples that have been used for faunal analysis. Approximately 0.5 mg sample material (e.g. 20-30 specimens of *G. bulloides,* 250 µm-500 µm) were crushed between glass plates to open the test chambers. Subsequently the samples were filled into vials. To remove contaminant phases the foraminiferal fragments were washed three times with distilled deionized water including ultrasonic cleaning for 2 minutes in-between the individual cleaning steps. The overstanding liquid was removed after each cleaning step. The samples were then washed with q methanol (Kuehnen et al., 1972) and ultrasonically cleaned for 2 min. followed by a cleaning step with distilled deionized water. To remove organic material the samples were treated with a hot oxidising $NaOH/H_2O_2$ solution (30 ml 0.1 N NaOH (p.a.) and 30 µl 30% H_2O_2 (suprapur)) for 30 min. During this procedure, the samples were cleaned ultrasonically for 2 min. every 10 minutes. Once again the samples were washed three times with distilled deionized water including ultrasonic cleaning for 2 minutes in-between the individual cleaning steps. The cleaned fragments were filled in vials, which were cleaned with 1 N q HCl

(Kuehnen et al., 1972), and dissolved by 0.1 N q HNO_3 (Kuehnen et al., 1972). Distilled deionized water was added to reach a minimum quantity of 1.5 ml needed for the Inductively Coupled Plasma-Atomic Emission Spectrometry (ICP-AES) analysis.

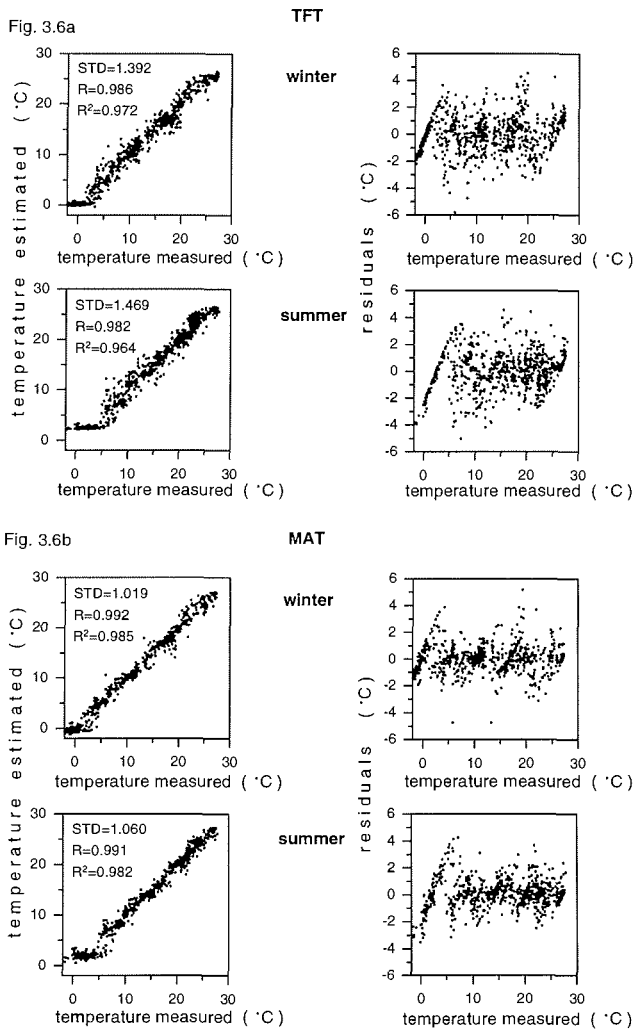

Fig. 3.6. Measured versus estimated SST obtained from the 721 sites of the North Atlantic database for transfer function technique (TFT) (Figure 3.6a) and modern analogue technique (MAT) (Figure 3.6b); R – correlation coefficient; STD – standard deviation; SST are calculated for the depth 0-50 m.

The samples were measured on a simultaneous ICP-AES (ISA Jobin Yion-Spex Instruments S.A. GmbH) selecting undisturbed and most intensive element lines (Mg: 279.55 nm; Ca: 317.93 nm; Y: 371.03 nm as internal standard). Elements were detected

by photomultipliers, whose tension was directly adapted manually for each element concentration. The long-term reproducibility of Mg/Ca is based on 312 analyses of a standard performed over a 3-years period. The standard deviation for Mg/Ca concentration is 0.124, standard error is 0.048. The temperatures were calculated by the species-specific calibration curve from Mashiotta et al. (1999) (Fig. 3.7).

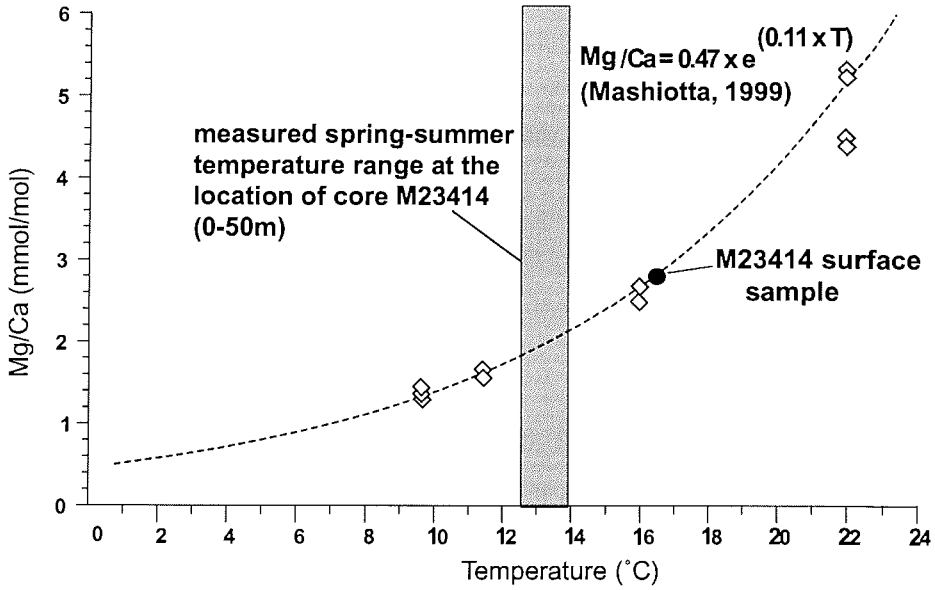

Fig. 3.7. Mg-temperature calibration curve from culturing experiments based on living *G. bulloides* taken from Mashiotta et al. (1999). SST calculated from the core tope sample and measured at M23414 core location spring-summer SSTs are indicated

3.2.4. Stable oxygen isotope measurements and IRD counts

Previous studies have indicated the advantage of applying more than one planktic foraminiferal isotope record to better understand past surface ocean changes (Deuser and Ross, 1989; Mulitza et al., 1997). This is why using only a single record some important paleoenvironmental information may be missed due to ecological preferences of the species selected (Bäckström et al., 2001). Therefore, stable isotope records in this study were produced from the polar species *N. pachyderma* (s) and from the temperate-subpolar species *G. bulloides*, also including the data generated by Jung (1996).

All isotopic analyses were made using a fully automated MAT 251 mass spectrometer (Leibniz Laboratory at Kiel University). Between 20-30 specimens of every species were taken from the 150-250 μm size subfraction for each isotope analyses. Measurements on *N. pachyderma* (s) for the Holocene section were mainly executed in 1 cm steps whereas 2.5 cm step interval was followed for the remaining core section. Measurements on *G. bulloides* were carried in 2 cm to 5 cm intervals.

In order to better interpret the climate changes deduced from the various surface ocean paleodata the IRD record was also considered. These lithic data were originally counted in the >250 μm size fraction and at 2.5 cm depth intervals.

3.3. Results

3.3.1. Planktic foraminiferal assemblage changes and their relation to millennial-scale climate variability

In the down core records seven main members comprise 88.8-100% of the total faunal composition (Fig. 3.8). Relative abundances of the other 14 species never exceed 2%, with a single exception of *Globorotalia truncatulinoides* dextral (d) which reaches up to nearly 6% during MIS 5.5, the marine analogue of the Eemian. The polar species *N. pachyderma* (s) strongly dominates the glacial core sections increasing to almost 100% during the most severe IRD events (i.e. IRD events number 1, 2, 3, 11, 14 and 15-16). The polar factor (Factor 1) is mainly described by this species thus tending to smooth all fluctuations above 50% level (Fig. 3.9).

Although *N. pachyderma* (d) is continuously distributed along the investigated interval, it prevails in the interglacial sections where it can reach up to 50%, e.g. during the Holocene and the Eemian (Fig. 3.8). This species exhibits a visual negative correlation with its left-coiling variety. Therefore, even subtle warming phases during glacial periods are marked by enhanced relative abundances. In the early glacial core sections, MIS 3 and early MIS 6, *N. pachyderma* (d) abundance is increased making up 12% and 28%, respectively. Despite a clear temperature preference, as expressed by Factor 2 (Fig. 3.9), this temperate to subpolar water species is found throughout the core, and even during the most severe IRD events its abundance makes up 3-5%. This feature is

well-known even from the Arctic ocean sediments (Bauch, 1999) and can be explained by the existence of two genotypes of *N. pachyderma* (d) that in fact belong to different species (Darling et al., 2001)

The distribution of *G. bulloides* and *T. quinqueloba* are described by Factor 4 and Factor 7 respectively (Fig. 3.9). Both species can tolerate a wide temperature range. They constitute a minor part of the glacial assemblage as well as interglacial assemblage but are increased during interstadial times (Fig. 3.8). Their abundances are more strongly reduced during pronounced cooling events, such as MIS 4 and the middle part of MIS 6, when they were absent and during peak interglacials the Eemian and the Holocene when they are mostly replaced by the warm-members of the assemblage. Interestingly, relative abundance of these species regularly increases immediately before IRD events.

Globorotalia scitula does not contribute to any factors, having a very low factor score in general. This species inhabits deeper water masses (Bé and Tolderlund, 1977; Barash, 1988) and occurs almost in all climatic zones, being adopted to a wide temperature range.

In contrast, *Globigerinita glutinata* and *G. inflata* are more abundant in the interglacial core sections but they also occur during the earlier part of MIS 6 and MIS 3 (Fig. 3.8). Although *G. inflata* is a single contributor to Factor 6, however, its low factor loading along the investigated core (Fig. 3.9) does not significantly influence the temperature estimates.

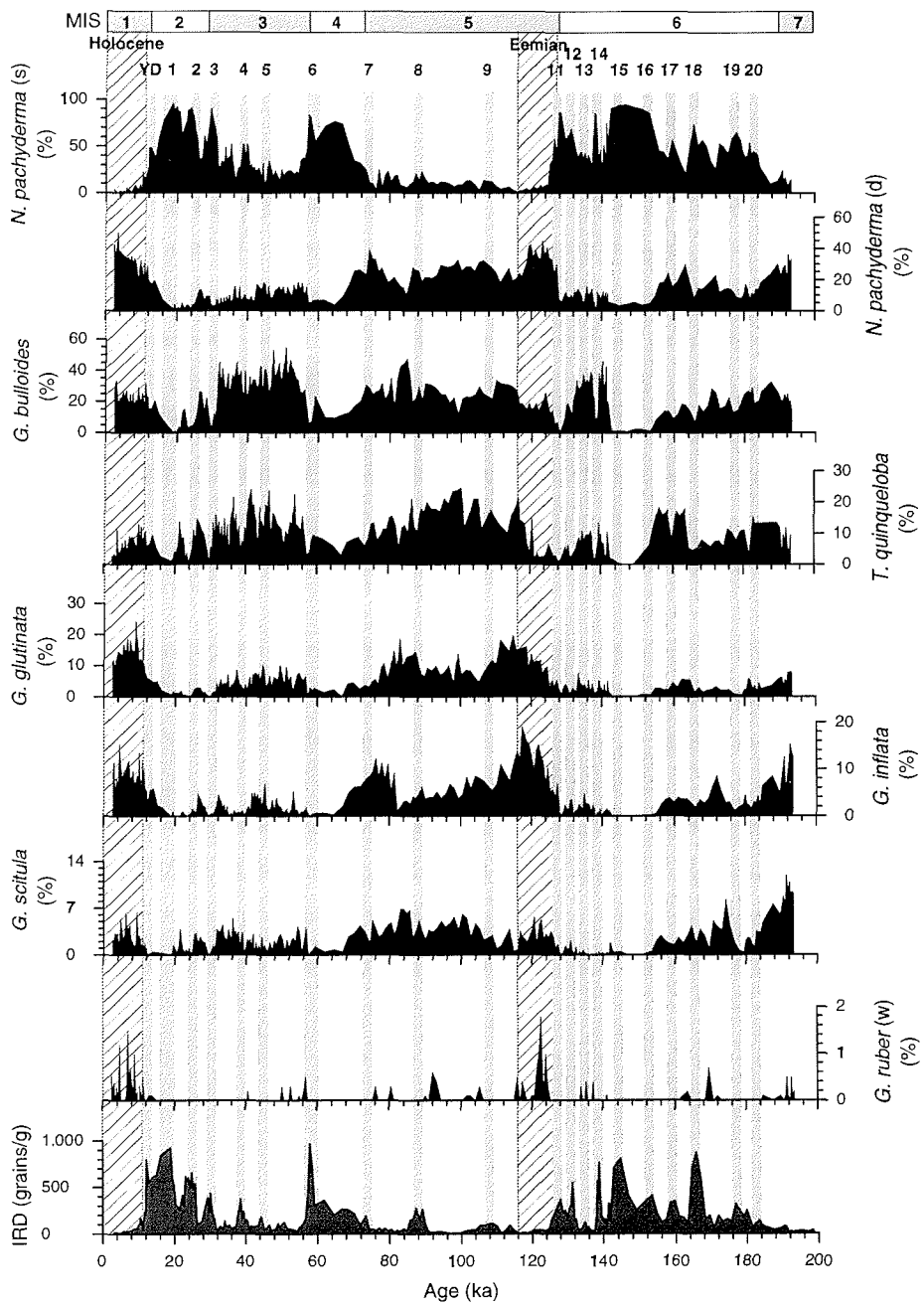

Fig. 3.8. Species distribution in core M23414 during last the two glacial-interglacial cycles. Marine isotope stage boundaries (MIS) are indicated. Numbered gray bars show IRD events; YD is Younger Dryas.

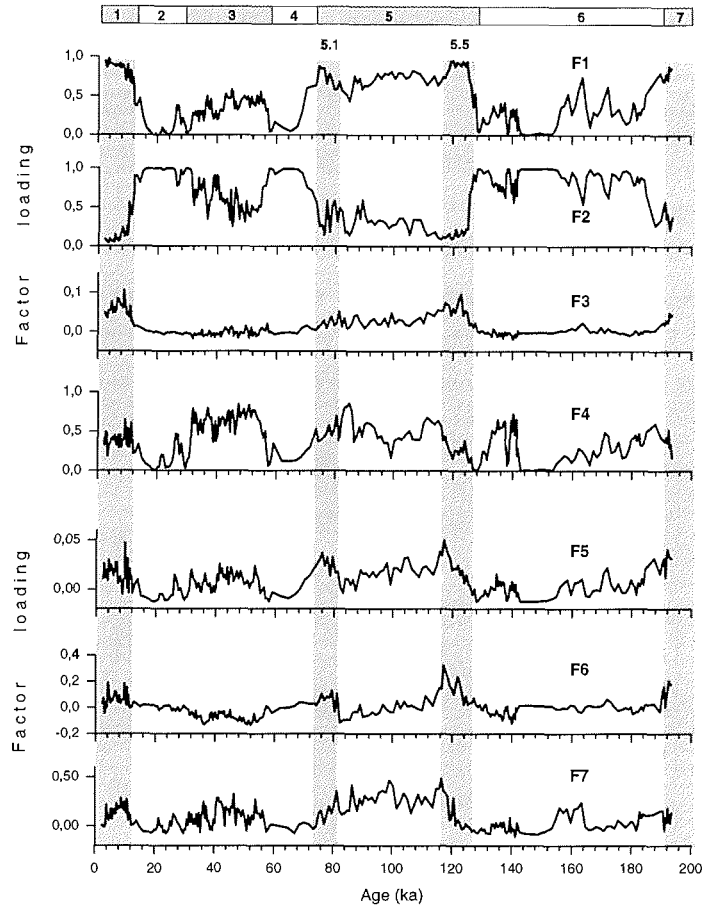

Fig. 3.9. Down core distribution of seven factors that were yielded by Principal Component Analysis. Marine isotope stage boundaries are indicated.

Special consideration must be given to relative abundances of rare species that are too low to contribute to temperature estimates but that can be extremely useful in tracing subtle short-term climate fluctuations indicating episodes of considerable temperature increase. Unfortunately, the common procedure that we have followed by counting 300 specimens per sample does not allow us to compare relative abundances of rare species quantitatively, since the standard errors in this case are comparable with the obtained range of relative abundances. However, even these data implicate that *G. ruber* (w), a typical tropical dweller, occurs not only during peak interglacial periods but also immediately after IRD events (Fig. 3.8).

3.3.2. SST variability inferred from faunal composition in comparison to isotope and IRD records

Core top temperature estimates generated by both methods using the foraminiferal census counts agree well with modern observed temperature (Levitus and Boyer, 1994) and show 10.4 and 14.0°C (MAT) and 11. 2 and 14.4°C (TFT) for winter and summer, respectively (Fig. 3.10). Both sets of paleoSST estimates also yield the same general trends and fine-scale structure revealing a high coincidence within the combined error of 2.4°C - 2.5°C for both seasons along the entire investigated core interval (Fig. 3.10).

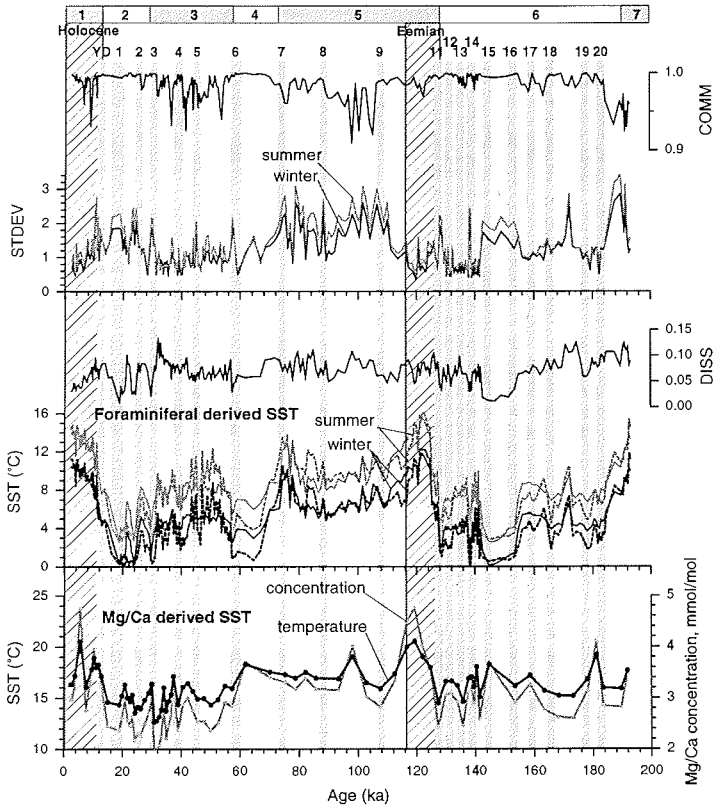

Fig. 3.10. Comparison of SST estimates based on different methods. Foraminiferal-derived SSTs are calculated for 0-50 m depth with two methods: MAT results are shown with solid lines and TFT results are shown with dashed lines, gray and black lines correspond to summer and winter temperatures, respectively. Peak interglacial conditions are indicated in hatched bars; Terminations are indicated in gray bars. Communalities (COMM) is the factor controlling SST estimates based on TFT; standard deviation (STDEV) of selected best analogues and dissimilarity index (DISS) provide information about precision of SST estimates derived from MAT.

Communalities and dissimilarity index, which controls consistency of the obtained results for TFT and MAT respectively, are always within acceptable range. The registered communality minimum along the investigated interval is 0.91 and the mean is 0.99 (Fig. 3.10). This clearly shows that all examined samples match well with the obtained model. The mean dissimilarity coefficient value is 0.07 (Fig. 3.10). The admissible value of dissimilarity coefficient depends on faunal diversity and can be determined empirically for every region (Overpeck et al., 1985; Waelbroeck et al., 1998). In our case, the dissimilarity coefficients calculated for M23414 core top sample and core top assemblages falling within the transitional zone do not exceed 0.14. Excess of this value would mean that selected best analogue samples do not really match with an analyzed one. Therefore, this value can be considered in our region as a threshold which separates foraminiferal communities adopted to considerably different climate conditions and can be used as an admissible value. In our records, dissimilarity coefficients are within the acceptable range, with the exception of the investigated part of MIS 7 (Fig. 3.10).

Standard deviations of the best selected analogues range from 0.4°C to 3.3°C (Fig. 3.10). Increased standard deviation values are not coincident with increased dissimilarity coefficients. For instance, the temperature minimum observed during MIS 6 between 144 and 156 ka is characterized by lowest dissimilarity coefficients but enhanced standard deviations that are related to the "cold-end" temperature problem when the summer temperature range -1.6 - 7.2°C is mostly characterized by the strong dominance of *N. pachyderma* (s).

The largest offsets between MAT and TFT results are obtained around 116 ka, 80 ka and between 56 and 68 ka. In all cases TFT estimates are as much as 2.5°C higher/lower from MAT results. This can be explained by the fact that TFT estimations are mostly driven by the interplay between polar and temperate factors that in turn are mainly determined by the distribution of *N. pachyderma* (s) and *N. pachyderma* (d), respectively (Fig.3. 9). Other species have very low factor scores (Table 3.1) in these factors and changes in abundances of predominant species are translated into temperatures with some overriding. Thus, when applying both approaches we obtain precise control on the generated temperature estimates. The advantage is also that both methods make use of the same database, since high offsets between SST generated by

MAT and TFT shown by previous researchers (Chapman et al., 2000) can also derive from differences in data bases they have used.

SSTs reach their maxima during peak interglacial conditions, the Eemian and the Holocene. The Eemian appears slightly warmer as it is marked by 16°C and 12°C for winter and summer, respectively which is 2°C higher than during the Holocene. Glacial temperatures are in general 8-9°C colder and reach their minima during the latest part of MIS 6 (between 144 and 156 ka) and during MIS 2 (between 20 and 24 ka) when 0°C and 3.5°C are registered for winter and summer, respectively. An additional minimum is observed during MIS 4 (between 56 and 66 ka) but this is shown only by TFT, probably due to shortcomings of this method, as already described above.

SST estimates based on foraminiferal diversity are in general agreement with planktic $\delta^{18}O$ (Fig. 3.11). Both *G. bulloides* and *N. pachyderma* (s) show considerable excursions of light isotope ratios during interglacial periods. However, $\delta^{18}O$ values of *N. pachyderma* (s) are much higher during the Holocene than during the Eemian, whereas *G. bulloides* $\delta^{18}O$ show insignificant differences during these two periods. However, *N. pachyderma* (s) better reflects short-lived climate fluctuations: every IRD event is preceded by an increase in $\delta^{18}O$ values that is coincident with an increase of the subpolar fauna and likely should be attributed to initial slight cooling. This increase is immediately followed by a light isotope excursion caused by meltwater input, as it is coincident with the IRD event.

For Terminations I and II, the SST estimates register a clear two-step structure, apparently caused by abrupt temperature changes during these major climatic transitions (Fig 3.10). Other short-term temperature fluctuations are registered along the entire investigated interval. They seem more pronounced during glacial times and interstadial intervals such as MIS 5.1-4. In contrast, during the Holocene and the Eemian, which represent peak interglacial conditions, these fluctuations are considerably reduced in amplitude. In general, most of those short-lived temperature oscillations are associated with IRD events (Fig. 3.11) that punctuate the entire time interval investigated, being absent only when peak interglacial conditions prevailed.

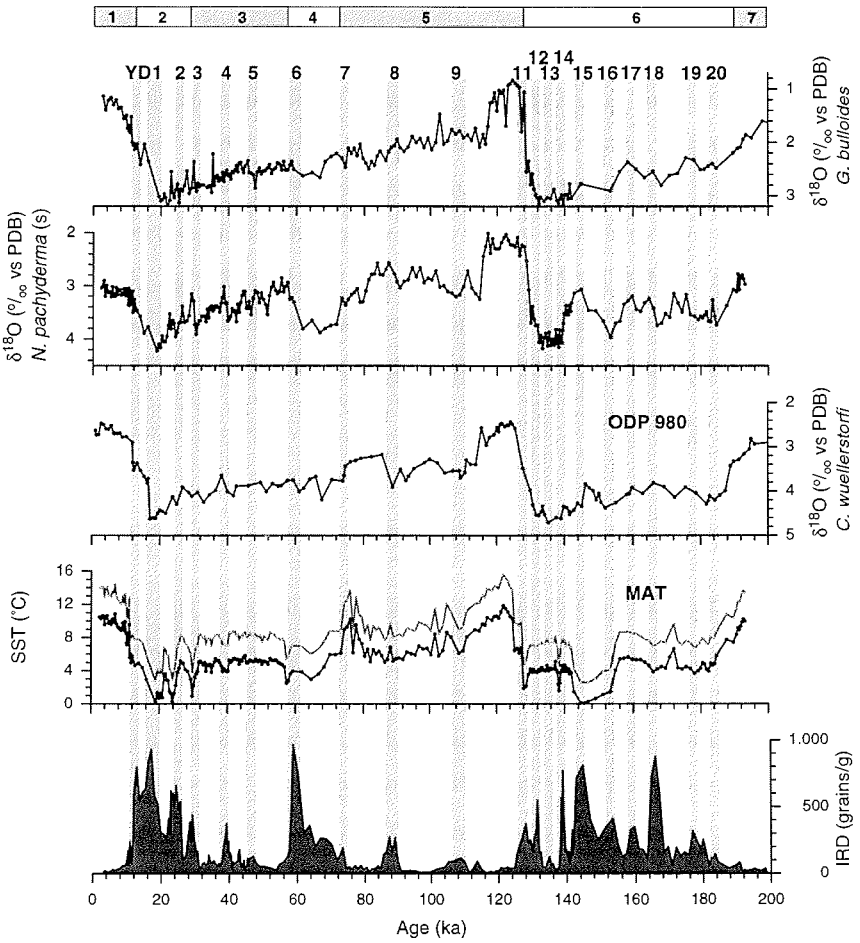

Fig. 3.11. Comparison of planktic isotope records performed on *G. bulloides* and *N. pachyderma* (s), foraminiferal derived SSTs (MAT) and IRD. Benthic isotope records from ODP 980 situated nearby are given to show an evolution of global ice volume (McManus, 1999). Numbered gray bars show IRD events; YD is Younger Dryas.

In comparison with the $\delta^{18}O$ record of *G. bulloides* millennial-scale variability is better expressed by the *N. pachyderma* (s) $\delta^{18}O$ record. This latter record shows that every IRD event is preceded by an increase in $\delta^{18}O$ which is followed by an immediate decrease coincident with enhanced IRD input.

3.3.3. Mg/Ca thermometry

The Mg/Ca concentrations measured on *G. bulloides* exhibit a temperature-dependent trend. The Mg/Ca-ratios show values between 2 and 4.8 mmol/mol with a glacial to interglacial amplitude of up to 2.7 mmol/mol. The glacial Mg/Ca-ratios vary between 2 and 4,2 mmol/mol with the lowest values noted during MIS 2. Interglacial peaks are marked by maxima in Mg/Ca ratio that increase up to 4.8 mmol/mol. Although, the Mg/Ca analysis resolution is not sufficient to trace millennial-scale variability, major IRD events are followed by a drop in Mg/Ca ratios of up to 1 mmol/mol.

3.4. Discussion

3.4.1. Comparison of the last two glacial-interglacial cycles

High resolution paleoceanographic records enable us to decipher and to compare in detail the climate evolution in the North Atlantic region over the two last glacial-interglacial cycles. Our results show that the Holocene and the last interglacial peak exhibit slight differences in climatic conditions which is indicated by faunal records as well as by isotopic records. The Eemian SSTs are as much as 2°C warmer. Significant difference in oxygen isotope value of *N pachyderma* (s) during interglacial peaks may be ascribed to extremely reduced abundance of this species during the Holocene. Probably this polar species, being adopted to the lower temperature range, represents the cold end of the Holocene SSTs and may not be regarded as an apposite temperature indicator for peak interglacial conditions in the middle latitude in general, as already shown by Bäckström et al. (2001). Interestingly, difference between the Eemian and the Holocene SSTs has been also registered in the North Pacific by alkenone-derived SST (Lyle et al., 2001) and in the South Atlantic by faunal-derived SST records (Hale and Pflaumann, 1999) and therefore seems to have a global character.

The investigated glacial periods display some more differences in their climate evolution. Marine oxygen isotope 6 appears to be the more severe glaciation than the last glacial period and is marked by a prolonged period of approximately 10 ka (between 144 and 156 ka) when temperature reached a cold level represented mainly by the polar species *N. pachyderma* (s) and accompanied only by an insignificant amount

of the right-coiling variety of this species, attributed to the same environmental group (Darling et al., 2001).

Planktic isotope records in the North Atlantic are complicated by meltwater overprint delivered from icebergs, thus masking possible temperature oscillations. So, neither *G. bulloides* nor *N. pachyderma* (s) isotopic records do indicate the prolonged cooling during MIS 6. However, both sets of foraminiferal-derived SSTs reach 0°C during the cold season and 3°C during the summer. As it is inferred from standard deviation values (up to 1.8°C and 2.2°C for winter and summer, respectively) obtained for MAT, this temperature minimum could be even lower in absolute value. As the core site M23414 was within polar waters during this time, implying that the Polar front was shifted far southward. It is interesting to mention that temperature during late MIS 6 was also estimated from tropical foraminiferal assemblages (McIntyre et al., 1989; Mix and Morey, 1996; Hale and Pflaumann, 1999), where it represents the coldest interval of the last four glacial-interglacial cycles, and is in agreement with temperature estimates from the eastern subtropical Pacific based on alkenone $U_k'^{37}$ (Lyle et al., 2001). As it is inferred from our data in comparison to benthic isotope records of ODP 980 (McManus et al., 1999) the SST minimum, occurring in MIS 6, led the maximum in global ice volume by more 5 ka. This implies that additional factors besides orbital forcing, e.g., the global carbon cycle (Shackleton, 2000), can be involved in driving the glacial-interglacial stage climate system. In contrast, during the last glacial period, SSTs repeatedly reached minima during short events of enhanced IRD input when large amounts of fresh water delivered from melting icebergs perturbed the thermohaline circulation. Moreover, absolute minimum temperatures occurred just prior to Termination I when global ice volume was largest.

Although Mg/Ca concentration values follow the main glacial-interglacial trend, temperature obtained from this analysis are apparently overestimated when compared with MAT/TFT. In the North Atlantic region, the subsurface dweller *G. bulloides* has a major bloom in April - June (Ottens, 1992). Therefore, SSTs calculated from Mg/Ca ratios are expected to reflect average spring-to-summer surface temperature values of the upper 0-50 m depth. The Mg/Ca-derived SST of the core top sample also deviates from modern observations (Levitus and Boyer, 1994) and faunal-derived SSTs by more than 2°C (Fig. 3.7).

It seems that the present Mg/Ca calibration is not optimal for our particular core location. Moreover, as the calibration used by us is based on culture-experiments that did not include the temperature range below 10°C (Mashiotta et al., 1999), it is also possible that along with temperature changes additional factors control the Mg-uptake of *G. bulloides*. Specimens obtained from plankton tows from the North Atlantic also show surprisingly high Mg/Ca-values (up to 13 mmol/mol), a finding that can not be attributed to temperature alone (Brown, 1996). Thus, applicability of this method to certain foraminiferal species including *G. bulloides* is still questionable (Müller, 2000; Elderfield and Ganssen, 2000) and needs an requires further assessment.

3.4.2. Abrupt climate changes

Millennial-scale SST variability is strongly expressed during glacial times and the temperate interglacial interval MIS 5.1-4. It also persists into peak interglacial periods, the Holocene and MIS 5.5, however, here diminished in their amplitude. Such a persistence was already described by previous researchers (Bond et al., 1997; Campbell et al., 1998; Oppo et al., 1998, 2001). During interstadials and glaciations these short-lived climate fluctuations are characterised by a considerable drop in SSTs of up to 3-5°C. They are always coincident with IRD events except periods of full interglacial conditions when IRD deposition almost ceased. Although our records do not show the characteristic SST decreases, which usually precede every IRD event (Bond and Lotti, 1995; van Kreveld et al., 2000), the short climate cooling episodes in our records can be inferred from positive excursions in *N. pachyderma* (s) $\delta^{18}O$ records that most likely were caused by decreases in SSTs. This finding is supported by distinct faunal changes: every major increase in *N. pachyderma* (s) abundance is led by excursions of *G. bulloides* and *T. quinqueloba* abundances, species that are able to tolerate cold temperatures. Because SST estimates obtained from the entire foraminiferal composition slightly smooth changes in relative abundance of individual species, resulting in a certain loss of some relevant information, the changes in these two species may be taken as good evidence of climate deterioration.

Slight decreases in SSTs, just prior to abrupt climate cooling with IRD, imply that the Laurentide ice sheet, which is considered to be the major contributor to IRD material

delivered to the North Atlantic (Gwiazda et al., 1996, Rasmussen et al., 1997), responded to initial climate cooling. Both paleoclimatic records and modelling experiments show that meltwater delivered from icebergs distorts thermohaline circulation (Oppo and Lehmann, 1995; Seidov and Maslin, 1999; Ganopolski and Rahmstorf, 2001), causing further cooling. The situation persists until freshwater input decreases and thermohaline circulation is initiated again. Occurrence of the tropical species *G. ruber* marks initial flushes of warm water. As this species also appears in between IRD events, it may be linked to the warm Dansgaard-Oeschger events. However, to prove that more accurate counts on this rare species are required in order to substantiate the interpretation.

By contrast to interglacial-glacial transitions that were developing gradually, glacial terminations occur as abrupt climatic changes. Our results have indicated a two-step deglacial process for both terminations which corroborates results of previous investigations (Jansen and Veum, 1990; Fronval and Jansen, 1996; Lototskaya et al., 1998, 1999) This all imply the existence of a threshold system that triggers climate changes during glacial-interglacial transitions (McManus et al., 1999).

3.5. Conclusions

Multiproxy paleoceanographic records have been obtained from a sediment core M23414, underlying the western edge of the North Atlantic Drift in order to examine the relationship between glacial-interglacial and millennial-scale climate fluctuations during the last two glacial-interglacial cycles. Paleotemperature estimates, derived from foraminiferal census data were calculated with both TFT and MAT methods using the largest available data base for the North Atlantic. The obtained results show high coincidence in absolute values and agree in general with planktic oxygen isotope records based on *N. pachyderma* (s) and *G. bulloides*. On the base of both SST records, the Eemian appears to be as much as 2 °C warmer than the Holocene at the studied site whereas the benthic $\delta^{18}O$ from a nearby core implies a global ice volume of a similar magnitude for these periods. In contrast, the evolution of last two glacial periods appears to be slightly different. In contrast to the last glaciation when the temperature minimum is coeval to the maximum of global ice volume, the temperature minimum in

MIS 6 is registered for the time when the ice sheets of the penultimate glacial period were still growing.

Millennial-scale climate oscillation reveal the same order of principal steps for both glacial-interglacial cycles. Each event starts with slight initial cooling which can be inferred from an increase in the abundance of subpolar species. The next step is marked by an IRD event coincident with a considerable SST drop of up to 3-5°C and terminates in an abrupt warming which brings the system back to the initial state. The amplitude of millennial-scale climate fluctuations was diminished during interglacial peaks. This is inferred from both decreased amplitude of SST oscillations and the absence of IRD. Oxygen isotope records of *N. pachyderma* (s) seem better to express millennial-scale fluctuations whereas its increased Holocene values do not reflect climatic conditions adequately. This indicates the advantages of using more than one isotope record for paleoclimatic reconstructions.

In order to assess the applicability of Mg/Ca thermometry performed on *G. bulloides*, temperature estimates derived from this method were compared with faunal SST results. Comparison revealed that Mg/Ca-derived SST follow the general glacial-interglacial trend. However, the considerable offset between the results implies that Mg/Ca temperature are largely overestimated and, probably, in addition to temperature other factors control Mg uptake in *G. bulloides* tests.

Implications of planktic foraminiferal size fractions for the glacial-interglacial paleoceanography of the polar North Atlantic

Abstract

Foraminiferal abundances derived from different mesh-size fractions were investigated from the polar North Atlantic for the time interval of the later part of marine oxygen isotope (MIS) 8 into early MIS 7 and the last 30 cal. ka in order to select the most representative fraction for paleoceanographic applications. The records cover the time interval with quite different glacial-interglacial climatic conditions. Whereas the interval of MIS 8-7 represents "intermediate" glacial-interglacial conditions, the younger core section characterizes more extreme climatic conditions consisting of the rather cold last glacial maximum (LGM) and the very warm Holocene.

The records from MIS 8 to 7 show that the larger size fractions (125-250 μm, >150 μm) reveal almost monospecific assemblages of the polar species *Neogloboquadrina pachyderma* sinistral (s) indicating a prevalence of cold polar-like surface water conditions during this time. By contrast, the smaller size fractions (100-150 μm, 80-150 μm) exhibit considerable increase of the subpolar species *Turborotalita quinqueloba*, which is representative of inflow of Atlantic water into the polar North Atlantic. In these smaller fractions the two species show a strong negative correlation with respect to changes in glacial-interglacial conditions. Although *T. quinqueloba* yielded sufficiently high numbers of total specimens in the two smallest fractions, which makes this species useful for interpreting temporal water mass alterations, the relative abundance changes in the 80-150 μm are twice as large as in the 100-150 μm fraction. Size fraction faunal analysis covering the last 30 cal. ka revealed occurrences of small-sized *T. quinqueloba* (80-150 μm) in the LGM interval, indicating seasonally open water conditions during this time. This finding demonstrates the advantage of employing small-sized fractions for paleoceanographic reconstructions of periods when relatively cold conditions prevailed in the Nordic seas.

4.1. Introduction

Because changes in the thermohaline circulation of the polar North Atlantic are regarded as an integral mechanism of climate modes over glacial-interglacial time scales (Rahmstorf, 1995; Broecker 1997), a profound knowledge of climate-related proxy tools at these latitudes is fundamental for reconstructing past environments. Planktic foraminiferal diversity is traditionally used as an important oceanographic proxy for such paleoenvironmental reconstructions. However, some difficulties arise when employing foraminiferal census data in regions such as the Greenland-Iceland-Norwegian seas (Nordic seas). At these high latitudes, foraminiferal counts executed on a mesh-size fraction >150 μm, as recommended by CLIMAP (1976), reveal only few subpolar species during peak warm periods (Kellogg, 1980). The number decreases dramatically during colder time intervals showing an almost monospecific foraminiferal assemblage that is dominated by the polar species *Neogloboquadrina pachyderma* sinistral (s). This monospecific assemblage makes it difficult to reconstruct past surface water properties and, in particular, to trace surface water mass inflow into the Nordic seas from the Atlantic during colder time periods.

Detailed studies on the biometry of tests of the dominant subpolar species in Nordic seas sediments, *Turborotalita quinqueloba*, have indicated that this species appears smaller under colder climatic conditions (Bauch, 1992). The results suggest the use of smaller mesh-size fractions to better interpret glacial and interstadial time intervals in the high-northern regions. Although it has been suggested that shortcomings of using smaller size fractions for foraminiferal counts may arise due to difficulties in the identification of juvenile tests and/or differential dissolution effects (Kellogg, 1984), the paleoceanographic potential of smaller mesh-size fractions has already been indicated (Marquard and Clark, 1987; Bauch, 1994; Hebbeln et al., 1994; Dokken and Hald, 1996).

The purpose of this study is to define the most representative foraminiferal size fraction that provides us with crucial information about water mass changes, in addition to other relevant climate data, such as iceberg-rafted debris (IRD) and stable oxygen isotopes, for reconstructing various glacial and interglacial conditions in the Nordic seas. The time span of Termination III and subsequent marine isotope substage (MIS) 7 was

chosen for a case study because previous investigations have shown this interval to be a weakly developed temperate period (Bauch, 1997). The results and methods are directly tested against comparable data from the radiocarbon-dated upper section of the sediment core that spans the last glacial maximum (LGM) and the much warmer Holocene.

4.2. Methods

4.2.1. Core position and present oceanographic setting in the Nordic seas

The site of the investigated cores is located on the eastern slope of the Iceland Plateau underlying the main pelagic sedimentation area of the Nordic seas (Fig. 4.1).

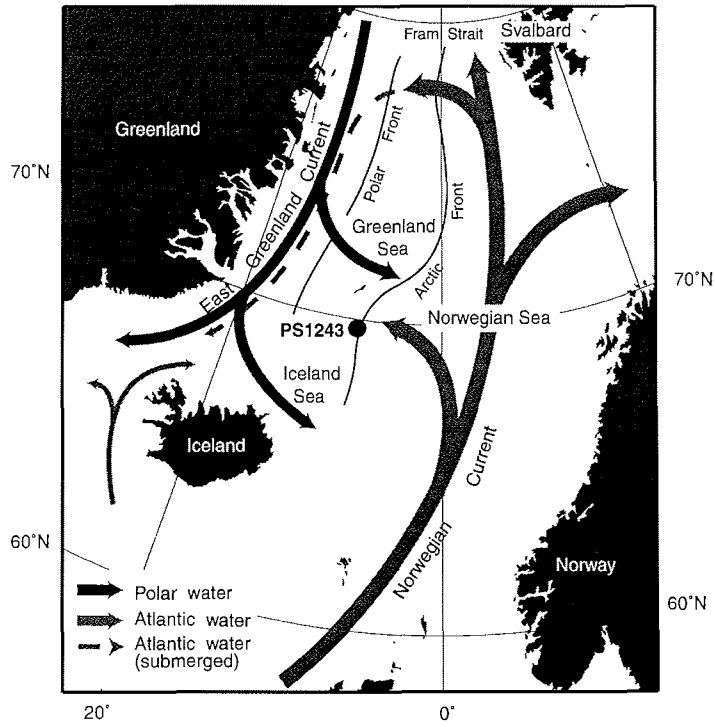

Fig.4.1. Core location and present day surface circulation in the Norwegian, Greenland and Iceland seas (Nordic seas) with oceanographic fronts subdividing the Nordic seas into different water masses; principal subdivision adopted from Johannessen (1986), Wadhams (1986), Mauritzen (1996).

The gravity core PS 1243-1 spliced with box core PS 1243-2 was selected for this study (Table 1.1).

Table 4.1. Geographical position and water depth of the investigated sediment cores.

Core	Latitude	Longitude	Water depth, m
PS1243-1 (G)	69.371 °N	06.540 °W	2710
PS1243-2 (B)	69.375 °N	06.540 °W	2716

B - box core, G - gravity core

The present surface circulation pattern in this region is characterized by the interaction between the northward-flowing temperate, saline Norwegian Current in the east, which is a continuation of the North Atlantic Drift, and the southward flowing cold, less saline East Greenland Current in the west. These two surface water masses, enclosed by the Arctic and Polar fronts, respectively, are separated by Arctic surface water, which is essentially a mixture of the other two watermasses (Fig. 4.1). The fronts can be recognized in surface sediments by a significant change in the relative and absolute abundances as well as by total calcium carbonate deposition (Johannessen et al., 1994). Hence, the selected core site is well-suited to reflect past changes in surface ocean circulation patterns.

4.2.2. Core stratigraphy and stable isotopes

The stratigraphic subdivision of core PS1243 is well-established and reaches back to MIS 12 (Bauch, 1997; Bauch et al., 2000b). Termination III (glacial-interglacial transition from MIS 8 to 7) and early MIS 7 is found above 460 cm core depth whereas the LGM and the Holocene intervals are recognizable within the upper 80 cm of the core (Fig.4.2a).

Stable isotope measurements were performed on the polar foraminiferal species *N. pachyderma* (s) using a fully automated MAT 251 mass spectrometer (Leibniz Laboratory at Kiel University). This species is conventionally used in northern regions due to its ubiquitous occurrence under both glacial and interglacial conditions. To reduce possible effects that may arise from measuring different morphotypes (Healy-Williams, 1992), 25-30 four-chambered specimens from the 125-250 μm size fraction were picked and analyzed. The measurements were executed at 1 cm intervals across Termination III, MIS 7 and MIS 2, and every 2 cm during the Holocene. All samples were originally taken as 1 cm thick sediment slabs.

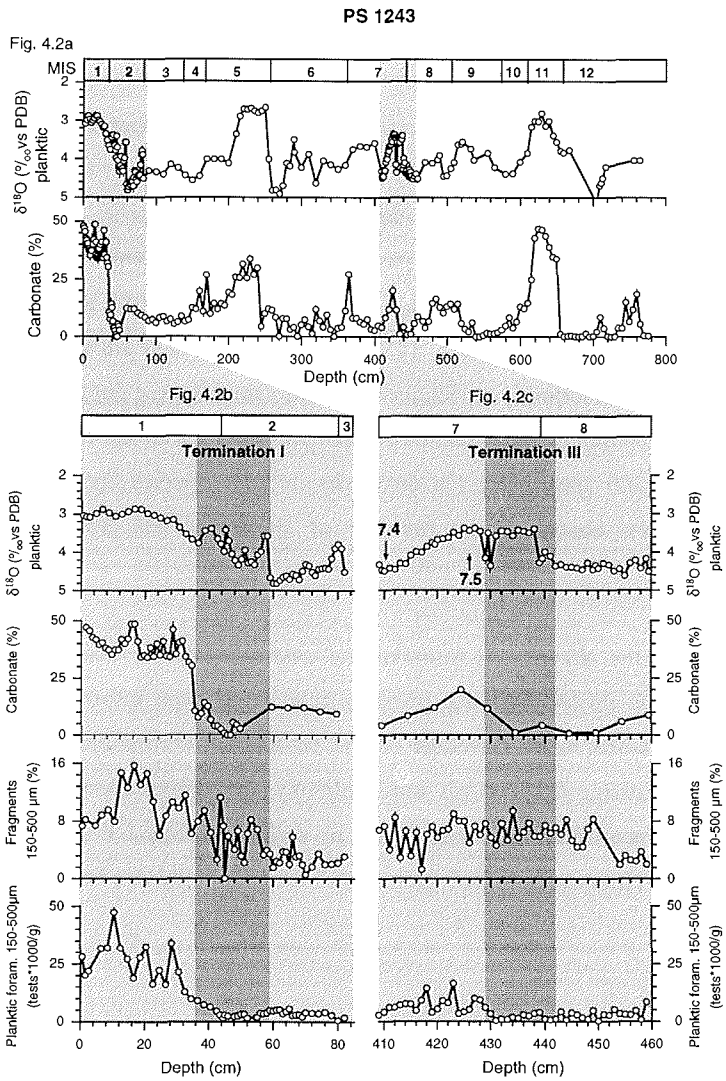

Fig. 4.2. Down core records of PS1243. Stratigraphic subdivision, as based on the $\delta^{18}O$ record of *N. pachyderma* (s) with marine isotope stage (MIS) boundaries, in comparison with the carbonate content (Figure 4.2a). Insets below show detailed records of the two investigated parts of the core, MIS 3-1 (Figure 4.2b) and MIS 8-7.5 (Figure 4.2c); relative proportions of test fragments are also shown in order to demonstrate possible dissolution along the investigated intervals.

The stratigraphy of the investigated upper core section is supported by 12 AMS radiocarbon dates (Bauch et al., 2001a). After subtraction of a reservoir age of 400 years and conversion of the radiocarbon ages into calendar years before present, the chronology of the upper 82 cm of the core reveals a time coverage of the last 30,000 calendar years (30 cal. ka).

4.2.3. Size fraction methods

All samples have been washed over a 63 μm mesh. The residues were then dried and sieved into different size fractions for further investigation. In order to find the optimum mesh size limits of foraminiferal counts with paleoceanographic implications, their relative abundance was determined separately on the size fractions 80-150 μm, 100-150 μm, 125-250 μm, 150-500 μm for time interval MIS 8-7. For the time interval MIS 2 and 1 the size fractions 80-150 μm, 125-250 μm, and 150-500 μm were compared; the overlap in the size fractions was obtained because samples were put together and sieved again. Prior to counting, each fraction sample was split by means of a microsplitter to approximately 300 specimens. On this basis, relative species abundance as well as foraminiferal test concentrations (number of specimens per gram sediment) were computed.

In addition to the changes in foraminiferal assemblages, the occurrence of IRD in sediments at the investigated site provides relevant climate information about major temporal fluctuation in ice coverage on the landmasses surrounding the Nordic seas. Moreover, comparing IRD records and stable oxygen isotopes allows interpretations of changes in surface water properties caused by meltwater (Bauch et al., 2001a). To take this information into account, IRD grains were counted in the size fraction > 250 μm.

4.3. Results

4.3.1. Dissolution effect

In the Nordic seas the carbonate component in the sediments is comprised primarily of biogenic component. Thus, the carbonate content can be taken as a rough proxy of foraminiferal test concentrations. This relation is particularly recognizable across glacial-interglacial transitions, such as Termination I and III, when the sedimentation of a major glacial phase changed from a hemipelagic to a dominantly pelagic depositional regime (Fig. 4.2b, 4.2c). The carbonate content and foraminiferal test concentrations remain low in these glacial and transitional intervals but they increase within the subsequent peak warm periods when relatively steady $\delta^{18}O$ values are found, indicating

a stable surface water regime. A significant difference between the MIS 1 and 7.5 is, however, recognizable in the actual values. These differences are stronger in MIS 1 than in MIS 7.5, supporting previous statements of a comparatively more pronounced climate warming in the Holocene.

It has been demonstrated that different planktic foraminiferal species vary in their susceptibility to carbonate dissolution (Berger, 1968; Le and Thunell, 1996), an effect that can considerably modify the proportion between species of a given assemblage. Moreover, because less calcified specimens are more sensitive to dissolution, control upon possible dissolution effects seems important when using smaller fractions for foraminiferal counts. In the studied core sections, the relative proportion of test fragments in the 150-500 µm size fraction of the two relevant core sections never exceeds 10 % and 15 %, respectively (Fig. 4.2b, 4.2c). These low values are in good agreement with previous investigations that revealed insignificant foraminiferal test corrosion in the Nordic seas during the past 300 cal. ka (Bauch and Helmke, 1999). Further evidence for a low dissolution index is indicated by the presence of translucent, thin-shelled juvenile tests that we have noted within the smaller size fraction samples.

4.3.2. Termination III and MIS 7

We concentrated on the proportions of polar species *N. pachyderma* (s) and subpolar species *T. quinqueloba* since their relative abundances change considerably in different size fractions. Because these two species are by far the most abundant over glacial and interglacial times, respectively, they show a strong negative correlation to each other (Bauch et al., 2001b). So-called "warm water" indicative subpolar species other than *T. quinqueloba* were neglected, as their abundances remain comparatively low in core PS1243, showing little change among the different size fractions for most parts of the two investigated time intervals.

When comparing foraminiferal diversity in the different size fractions, the relative abundance of the subpolar species *T. quinqueloba* exhibits a gradual increase towards the smallest fraction (Fig. 4.3). In the coarsest fraction this species occurs during the main warming event MIS 7.5 and shows only one minor spike during the preceding Termination III. In both cases, the relative abundance remains well below 10 %. Within

the 125-250 µm fraction these two spikes are also apparent, but their actual values increase insignificantly. However, in both of the smaller fractions *T. quinqueloba* is present in the entire interval including the termination. On the basis of the 80-150 µm fraction its relative abundance rises to nearly 60 % within the peak interglacial (425-420 cm core depth) and up to 40 % in the glacial part of MIS 8. Thus, the smallest investigated fraction exhibits the highest abundance of *T. quinqueloba.*

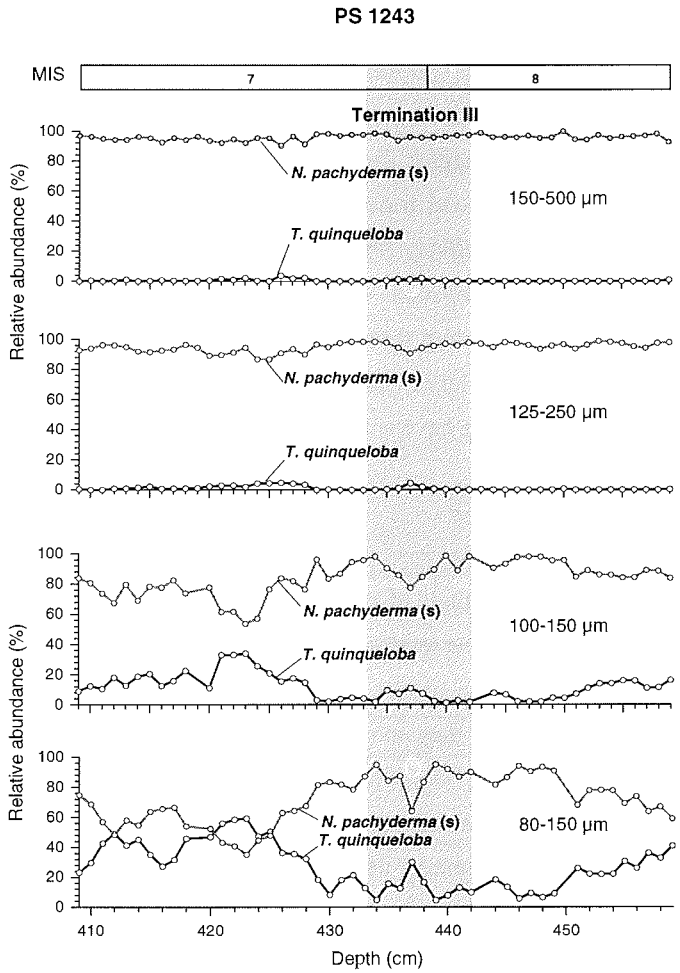

Fig. 4.3. Comparison of relative abundance records of *T. quinqueloba* and *N. pachyderma* (s) in different mesh-size fractions from MIS 8 across Termination III and through early MIS 7.

The section that we identify as MIS 7 having interglacial character can be separated from Termination III on the basis of low oxygen isotope values combined with low

IRD, increased foraminiferal concentrations and increased relative abundance of *T. quinqueloba* (Fig. 4.4). On a glacial-interglacial comparative basis, this subpolar species reveals an inverse correlation with IRD. Such a correlation seems to persist also during the glacial-interglacial transition where there are several events showing enhanced IRD content and low *T. quinqueloba* relative abundance. One of these events occurs between 450 and 440 cm, in the early transition, and another between 435 and 428 cm core depth. This second event is also associated with a prominent excursion in the oxygen isotope record.

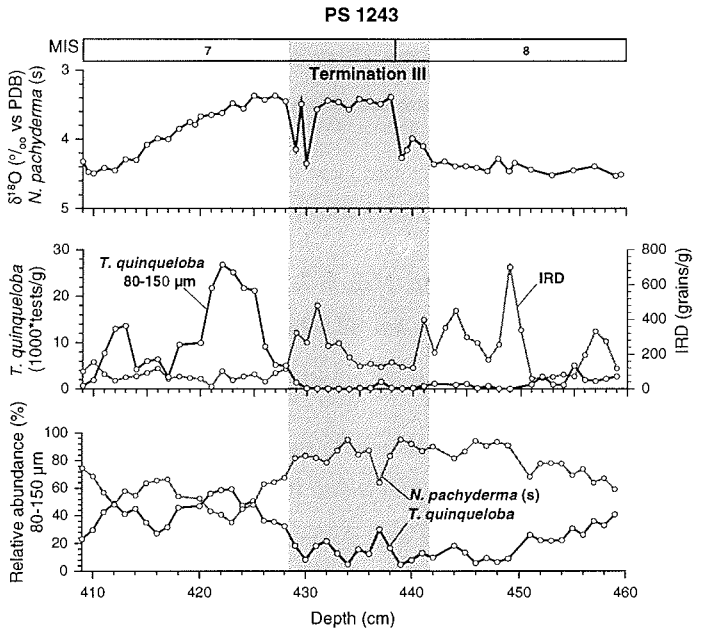

Fig. 4.4. Relative abundances of *T. quinqueloba* and *N. pachyderma* in the 80-150 µm fraction in comparison with records of planktic $\delta^{18}O$ and iceberg debris (IRD) during Termination III and early stage 7.

In general, the changes seen in the $\delta^{18}O$ record of the termination are also reflected in the foraminiferal assemblage which indicate a slight surface warming centered at 437 cm core depth. The $\delta^{18}O$ values in this interval are already as low as in early substage 7.5, but the relative numbers of subpolar foraminifera in the termination remain much lower. Because IRD deposition was also still higher than during subsequent substage 7.5, sea surface conditions between 438 and 431 core depth were probably affected by meltwater input that became superimposed on the $\delta^{18}O$ values. Although it is difficult to distinguish sea surface warming from salinity lowering due to meltwater input in the

$\delta^{18}O$ record, the fluctuations in *T. quinqueloba* ranging between 5-20 % seem to indicate more complex surface water conditions during Termination III than indicated by IRD and $\delta^{18}O$.

Towards the end of the deglaciation the strong decrease of IRD coincides with a growing abundance of *T. quinqueloba* (Fig. 4.4). Within the section having low IRD the relative abundance of *T. quinqueloba* reveals two main peaks with values of 60% and 50%, respectively. These peaks are separated from each other by a significant decrease centered at 416 cm core depth which coincides with a slight increase of IRD. Interestingly, the $\delta^{18}O$ record does not show such fluctuations; instead, it reveals a gradual increase after lowest values are found between 428 and 425 cm core depth.

4.3.3. The last 30 cal. ka

To better evaluate the results from MIS 8-7, planktic foraminiferal diversity was determined for the fractions 150-500 µm, 125-250 µm, and 80-150 µm also for the time interval of the LGM and the Holocene (Fig. 4.5).

The relative abundances of *N. pachyderma* (s) and *T. quinqueloba* across the last 30 cal. ka display an almost inverse correlation for all three size fractions. In the >150µm and >125µm fractions *N. pachyderma* (s) dominates during the LGM and most of Termination I until it is largely replaced by *T. quinqueloba* at about 10 cal. ka, concomitant with the cessation of IRD deposition.

During MIS 2, which is usually considered the phase of most severe cooling during the last glaciation, the presence of *T. quinqueloba* in the two larger size fractions is sparse. Only at 13.5 cal. ka is there a significant increase of up to 20%. This event seems related to the Bølling/Allerød period (Bauch et al., 2001a). In the smallest size fraction, however, *T. quinqueloba* is continuously present. Interestingly, it shows not only an abundance peak during the Bølling /Allerød period, where it reaches 41%, it also reveals an enhanced abundance between 24.5 and 18 cal. ka. This increase in abundance of up to 24% is concurrent with a strong increase of IRD and occurred at a time when both benthic and planktic foraminifera usually show highest $\delta^{18}O$ values due to the largest volume of global ice.

After cessation of IRD deposition, which marks the end of significant freshwater input due to melting icebergs, the abundance of *T. quinqueloba* rises steeply up to 70% within the two smallest size fractions. As in MIS 7, this species shows the lowest value (up to 45 %) in the largest size fraction. But all these fractions reveal a time-coeval increase

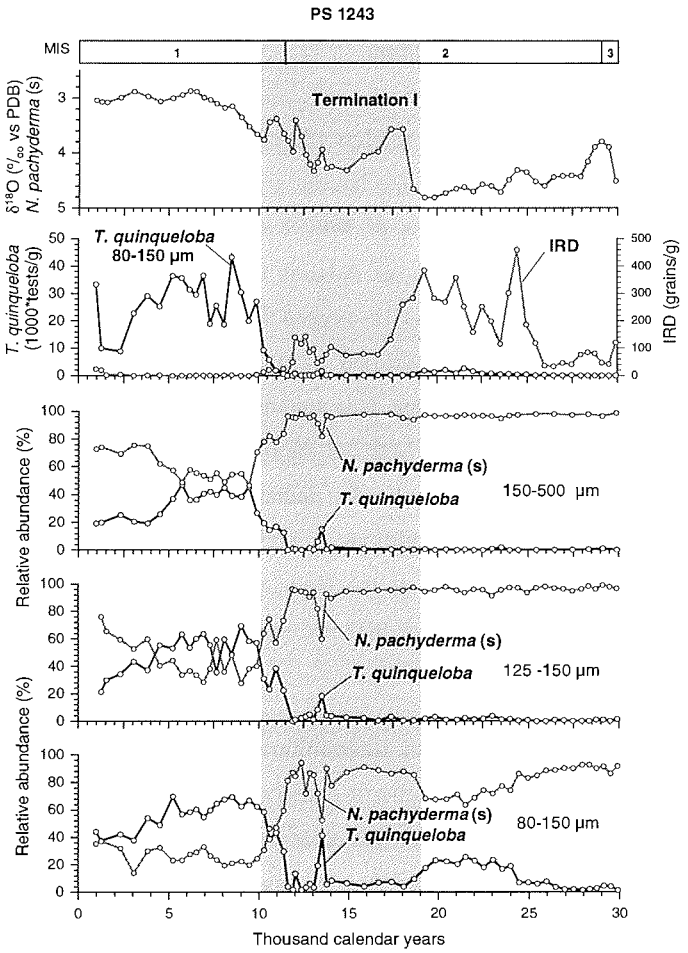

Fig. 4.5. Relative abundances of *T. quinqueloba* and *N. pachyderma* in different size fractions during the last 30 cal. ka, in comparison with records of planktic $\delta^{18}O$ and iceberg-rafted debris (IRD).

during the warmest phase of the Holocene which commenced in core PS1243 in the Nordic seas after 10 cal. ka. The end of the Holocene 'climatic optimum' started between 5 and 6 cal ka and is recognizable in all records of *T. quinqueloba*. A significant difference is found in the 80-150 µm record of *N. pachyderma* (s), which exhibits a more gentle increase than *T. quinqueloba* after 5 cal. ka due to a considerable

increase of *Globigerinita glutinata* and an additional appearance of the small-sized subpolar species *Globigerinita uvula*.

4.4. Discussion

4.4.1. Paleoceanographic reconstruction

By contrast to time intervals such as the last 150 cal. ka, little is known in detail about climatic conditions during MIS 7 in the Nordic seas as well as in the North Atlantic. The three oxygen isotopic subevents of MIS 7 (Martinson et al., 1987) that show relatively similar SSTs for the Northeast Atlantic region (Ruddiman et al., 1986b) are also recognizable in the Nordic seas in oxygen isotope records. However, only the oldest event MIS 7.5 could be identified as an interval exhibiting some kind of interglacial-like conditions on the basis of the occurrence of subpolar foraminifera (Bauch, 1997). The assumption that MIS 7.5 may have been the warmest interval for MIS 7 in the northern hemisphere can be also deduced from certain terrestrial data (e.g., Winograd et al., 1992). That the conditions in MIS 7.5 were considerably colder than during a proper interglaciation such as the Holocene was clearly confirmed by us on grounds of continuous occurrences of IRD and the foraminiferal data from the coarser size fractions.

But the minor fluctuations of planktic foraminiferal records in the size fractions >125 µm do not allow us to decipher details of climatic change for this time interval. The record of the smaller size fractions, on the other hand, provide more such information. This shows that the process of deglaciation during Termination III developed in steps accompanied by variations in iceberg discharge, probably due to fluctuations in the size of glacier ice that surrounded the Nordic seas. The melting of these icebergs and the resulting lowering in surface salinity must have affected deep water formation processes in the Nordic seas (e.g., Rahmstorf, 1995). It seems very likely that the meltwater output during Termination III also left its mark on the water mass circulation in the subtropical northeast Atlantic where similar climate-related variability has been described (Sarnthein and Tiedemann, 1990).

Because *T. quinqueloba* exhibits such a visual inverse correlation with IRD, sea-ice cover and lowered salinity due to freshwater from melting icebergs appear to be major

environmental factors for its thriving in the Nordic seas. The persistent although reduced presence of IRD during the peak of MIS 7.5 suggests that lowered salinity was the main reason for the restricted abundance of *T. quinqueloba* during this interval. It has been suggested previously that the water structure bioproductivity could influence the distribution of *T. quinqueloba* (Loubere, 1981; Johannessen et al., 1994). Although the ecological preferences of this species are not yet clear, it seems evident that its main use in the Nordic seas is as a proxy for Atlantic water input. Recent investigations for the water column confirm this by showing that *T. quinqueloba* follows the main body of Atlantic water masses, which is generally characterized by increased salinity, temperature, and bioproductivity (Carstens et al., 1997).

Using the analogue approach by comparing the data from MIS 8-7 with those of the last 30 cal. ka does not make it easier to determine more precisely the specific surface water conditions during MIS 7. This is because in both MIS 2 and the Holocene the systematics behind the proportions of small and large number of tests do not really match with MIS 7.5. Apart from the Bølling/Allerød warming event reflected by a significant increase of *T. quinqueloba* abundance in all size fractions investigated, the presence of this subpolar species may indicate an enhanced input of Atlantic surface waters during the LGM, which was previously identified as a severe cooling phase with perennial ice cover in the Nordic seas (CLIMAP, 1976).

Based on the discovery of small-sized *T. quinqueloba* during the LGM, which are detected in the Fram Strait and the southern Nordic seas (Bauch, 1992; Hebbeln et al., 1994; Dokken and Hald, 1996), SSTs and $\delta^{18}O$ time-slice reconstructions (Schulz, 1994; Weinelt, 1996), seasonally open water conditions are now widely accepted to have existed in the Nordic seas during the LGM. Moreover, the occurrence of such small-sized subpolar specimens during the LGM has been recently explained with a subsurface inflow of Atlantic water masses (Bauch et al., 2001a), similar to the conditions found today in the southeastern Arctic Ocean and Fram Strait. In this polar region, small tests of *T. quinqueloba* are quite abundant in the water column, but only within the Atlantic-derived water that is advected beneath a cold and low-salinity surface layer (Carstens et al., 1997).

In the surface sediments underlying the polar waters of the western Nordic seas, the abundance of *T. quinqueloba* is scarce (Johannessen et al., 1994), presumably because

of enhanced calcite corrosion (e.g., Bauch et al., 1999). For the two intervals investigated at the site of core PS1243, all our results indicate that dissolution affecting the assemblage composition in the smallest size class is not a major issue. More likely causes are circulation schemes with quite a different surface water structure. It is thus concluded that the low abundance of large-sized specimens of *T quinqueloba* during MIS 7 resulted from advectional processes that preferentially transported smaller specimens farther than larger tests.

4.4.2. Which size fraction to choose in high-latitude foraminiferal studies?

Questions about the most representative size fraction have been discussed by many authors, as the relative abundance of foraminiferal species shows a strong dependence on mesh size selection (Berger, 1971; Bé and Hutson, 1977; Kellogg, 1984; Brummer, 1988; Peeters et al., 1999). Large data sets were collected from surface sediments during the last three decades using a lower size limit of 150 µm (Imbrie and Kipp, 1971; Prell, 1985; Pflaumann and others.,1996). Therefore, this mesh size is also used for downcore planktic foraminiferal census counts that form the basis for past sea surface temperature (SST) reconstructions. However, our investigation clearly demonstrates that in high latitudes this size fraction can not be employed for paleoclimatic reconstruction of time intervals colder than very warm extremes, such as the Holocene, due to low foraminiferal diversity.

A new approach to SST reconstructions, developed especially for high latitudes, still shows uncertainty in the crucial low temperature range that is so relevant for reconstructing glacial climates; i.e., from approximately 3°C to the freezing point of sea water (Pflaumann et al., 1996; Weinelt et al., 1996). As indicated by our results this deficiency is due to foraminiferal counts executed on fractions with a lower size limit of 150 µm and 125 µm, that reveal an almost monospecific assemblage represented by *N. pachyderma* (s) even for a relatively temperate time interval (Fig. 4.3). Because at polar latitudes warm phases such as the Holocene were the exception rather than the rule during the past 450 cal. ka (Bauch, 1997), the large mesh sizes are clearly unsuited to provide climatic details of periods with colder than peak interglacial temperatures.

In our records, the smaller mesh sizes yield different proportions of foraminiferal species due to a gradual increase of the relative abundance of *T. quinqueloba* from the largest to the smallest size fraction where it largely replaces *N. pachyderma* (s). Because in some foraminiferal species, including *T. quinqueloba*, the average test size may change as a function of environmental conditions (Malmgren and Kennett, 1976; Kroon et al., 1988; Bauch, 1994), a smaller test size could also reflect ecological stress caused by adverse circumstances, such as low water temperatures.

N. pachyderma (s) is the only polar species adopted to very low water temperatures (Bé and Tolderlund, 1971). Paleoceanographic studies have shown that even a minor increase of *T. quinqueloba* abundance in Nordic seas sediments may be taken as good evidence of an inflow of temperate waters from the North Atlantic. Thus, under circumstances when no other markers for an input of North Atlantic surface water exist, small-sized *T. quinqueloba* can serve as a tool for paleoclimatic reconstructions. But to establish a quantitative link between planktic foraminiferal assemblages based on small size fractions and SST cannot be taken for granted. This is because other factors, for instance, primary production and the position of oceanic fronts dividing different water masses, may also have a profound influence on the geographical distribution of small-sized foraminiferal assemblages (Johannessen et al., 1994; Carstens et al., 1997).

Foraminiferal diversity in smaller size fractions are clearly more sensitive to dissolution due to the higher number of juvenile, less calcified specimens. Although the perennially ice-free areas of the Nordic seas have basin depths above the carbonate compensation depth showing relatively high carbonate deposition today (Johannessen et al., 1994), control of dissolution effects still needs to be taken into account when evaluating fossil foraminiferal assemblages. Both smaller fractions investigated have yielded sufficient numbers of specimens of *T. quinqueloba* to recognize an input of Atlantic water, but the relative abundance of this species in the 80-150 µm fraction is nearly twice as much as in the 100-150 µm size fraction. Consequently, the 80-150 µm fraction can be considered more sensitive in detecting and interpreting water mass changes in time intervals when larger size fractions do not show sufficient numbers of *T. quinqueloba* specimens. The foraminiferal counts of different size fractions from the last 30 cal. ka indicate that the larger size fractions are sufficient to unveil climate variability of extreme interglacial periods. By contrast, to characterize climate conditions of time

intervals having considerably colder conditions than the Holocene, it is necessary to include the smaller size fractions in paleoceanographic interpretations.

4.5. Conclusions

Foraminiferal abundances derived from different mesh-size fractions were investigated from the central Norwegian sea for the time interval of MIS 8-7 in order to determine the most representative fraction for paleoceanographic applications. The method was also tested against comparable data from the radiocarbon-dated upper section of the core that spans the LGM and the Holocene. Results from MIS 8/7 show that large size fractions (>150 µm, 125-250 µm) conventionally taken for faunal analysis reveal an almost monospecific assemblage represented by the polar species *N. pachyderma* (s), whereas smaller fractions (100-150 µm, 80-150 µm) exhibit considerable increases of subpolar species *T. quinqueloba* with up to 60% in the smallest fraction during MIS 7.

A clear inverse correlation between *T. quinqueloba* abundance and IRD during Termination III implies that salinity is probably one of the major environmental factors controlling the occurrence of this species in the Nordic seas. Although a direct link between foraminiferal composition in the small-sized fraction and SST is probably hampered by the influence of several other factors, fluctuations in the faunal data also indicate significant changes in sea surface properties for comparatively cold time intervals when other more traditional paleoceanographic tools seem less sensitive to record climate-driven water mass changes. Based on the small-sized *T. quinqueloba* records in combination with IRD, it can be concluded, that the process of deglaciation during Termination III was developed in steps, possibly in accordance with fluctuations in the size of glacier ice that around the Nordic seas. Our results from the last 30 cal. ka also reveal a simultaneous occurrence of small-sized *T. quinqueloba* and IRD during the LGM. They serve as evidence for partially open water conditions and point to a subsurface advection of Atlantic water into the Nordic seas during this time. Because this signal is registered neither in the $\delta^{18}O$ records nor in the foraminiferal counts executed on the larger fractions, including small-sized *T. quinqueloba* in interpreting proper glacial conditions seems appropriate.

Both smaller fractions investigated have yielded sufficient numbers of specimens of *T. quinqueloba* to allow for a paleoceanographic reconstruction. However, the smallest

fraction 80-150 µm seems the more sensitive one, as it reveals relative abundances that are considerably higher than in the mesh-size100-150 µm. Thus, for high-latitude studies of glacial-interglacial sediments there is no need to lower the size limit below 80 µm as this would hampers the efficiency of foraminiferal counting procedures unnecessarily.

Acknowledgments

We thank the shipboard crew and scientists of RV Polarstern for collecting the sediment cores used in this study. We are also grateful to an anonymous reviewer's comments which helped to improve the manuscript. The study was funded by the German Research Foundation (DFG, Grant no. Schm 250/49).

5. Conclusions

The rational of this study was to trace late Quaternary climatic changes in the high-northern latitudes on glacial-interglacial as well as millennial time scales using foraminiferal census data from two sediment cores to infer from them sea surface temperatures as the principal tool for paleoceanographic reconstructions. These results were supported by stable isotope measurements performed on planktic foraminifers and iceberg-rafted debris (IRD) records. This thesis compiles three separate manuscripts, dedicated to different paleoclimatological problems in the temporal and sediment subpolar North Atlantic regions.

In the North Atlantic, SSTs for the last five glacial-interglacial cycles (past 500,000 years) were calculated with both TFT and MAT. Foraminiferal based SSTs in the North Atlantic were also compared with Mg/Ca thermometry inferred from the planktic foraminiferal species *G. bulloides* derived from the same core. Faunal analyses and SST records were examined in detail which results in conclusions summarized below:

- Generally diminished intra-interglacial climate variability was found in all major interglacial periods.
- The warmest conditions, characterized by summer SST increases of up to 16°C, were registered for MIS 5.5.
- The Holocene and MIS 11 and MIS 13 are marked by slightly colder (up to 2 °C) than Holocene's SST values.
- Although SSTs during MIS 7 and 9 yield very similar values to Holocene's ones the enhanced dissimilarity coefficient derived from MAT implies that the obtained results may significantly deviate from real values.
- As it is inferred from detailed analyses of foraminiferal abundances, the SST values, obtained for MIS 7, appear largely overestimated. The enhanced abundances of subpolar species, especially *T. quinqueloba* indicate proximity of the polar front.
- Along the entire investigated abrupt climatic changes exhibit the same order of principal steps, starting with a slight initial cooling, which leads to an IRD event coincident with considerable cooling followed by abrupt warming that brings the climate system to the initial state.

- Frequency and intensity of IRD events, related to abrupt climatic changes, strongly reveal a dependency on the particular climatic mode. Periods with diminished climatic contrasts are characterized by less frequent and less severe IRD deposition.
- Changes in Mg/Ca ratio of *G. bulloides* in the northeast Atlantic reflect a temperature signal which, however, seems to be largely overestimated. Thus, calibration of this method needs further improvement.

In the Nordic seas foraminiferal abundances in different size fraction were investigated during MIS 8-7 in order to determine the most representative fraction for paleoceanographic applications in this region. The obtained results were tested against the well-investigated upper section of the core which covers the last 30,000 years.

- In polar waters the small-sized fractions, 80-150 µm and 100-150 µm, appear to be useful for paleoceanographic reconstructions due to enhanced abundance of subpolar species *T. quinqueloba*.
- Relative abundance of *T. quinqueloba* in the small fractions reveal pronounced fluctuations as the result of temporal Atlantic surface water input. This proposes small sized *T. quinqueloba* as a marker of short-lived climatic fluctuations in North polar environments.
- A clear negative correlation between *T. quinqueloba* abundance and IRD records implies that salinity may be a major environmental factor controlling its occurrence in the Nordic seas.
- As inferred from *T. quinqueloba* abundance and IRD occurrence, the process of deglaciation during Termination III was developed in several steps.
- Coincidence of IRD occurrence and significant increase of abundance of small-sized *T. quinqueloba* during LGM indicate partially water opened conditions and allow to speculate about subsurface pattern of the Atlantic water advection.

The obtained results reveal a complex relationship between glacial-interglacial variability and millennial-scale surface water changes in the polar and subpolar North Atlantic regions. It could also be shown that foraminifers are an extremely useful group in paleoceanographical investigations and that detailed faunal analyses help to assess and interpret SST results derived from foraminiferal counts. However, for more even successful paleoclimatic reconstructions further investigations and improvements in

foraminiferal analyses are needed. This should include consideration of rare species as well as smaller mesh-sizes, where necessary.

References

Augstein, E., Hempel, G., Schwarz, J., Thiede, J., and Weigel., W., 1984, Die Expedition Arktis II des FS "Polarstern" 1984 mit Beiträgen des FS "Valdivia" und des Forschungsflugzeuges "Falcon 20" zum Marginal Ice Zone Experiment 1984 (MIZEX): Reports on Polar Research, v. 20, 192 p.

Bäckström, D. L., Kuijpers, A., and Heinemeier, J., 2001, Late Quaternary North Atlantic paleoceanographic records and stable isotopic variability in four planktonic foraminiferal species: Journal of Foraminiferal Research, v. 31, p. 25-31.

Barash, M. S., 1988, Quaternary paleoceanography of the Atlantic Ocean: Moscow, Nauka (in Russian), 272 p.

Bard, E., 2001, Comparison of alkenone estimates with other paleotemperature proxies: Geochemistry, Geophysics, Geosystems, v. 2, paper number 2000GC000050.

Bauch, H. A., 1992, Test size variation of planktic foraminifers as response to climatic changes: International Conference on Paleoceanography (ICP IV), p. 56.

Bauch, H. A., 1994, Significance of variability in *Turborotalita quinqueloba* (Natland) test size and abundance for paleoceanographic interpretations in the Norwegian-Greenland Sea: Marine Geology, v. 121, p. 129-141.

Bauch, H. A., 1997, Paleoceanography of the North Atlantic Ocean (68°-76°N) during the past 450 ky deduced from planktic foraminiferal assemblages and stable isotopes, *in* Hass, H. C. and Kaminski, M. A., eds., Contributions to the Micropaleontology and Paleoceanography of the Northern North Atlantic, Krakow, Grzybowski Foundation Special Publication, p. 83-100.

Bauch, H. A., 1999, Planktic Foraminifera in Holocene sediments from the Laptev Sea and the central Arctic Ocean; species distribution and paleobiogeographical implication, *in* Kassens, H., Bauch, H. A., Dmitrenko, I. A., Eicken, H., Hubberten, H. W., Melles, M., Thiede, J., and Timokhov, L. A eds., Land-ocean systems in the Siberian Arctic; dynamics and history, Berlin, Springer, p. 601-613.

Bauch, H. A., and Helmke, J. P., 1999, Glacial-interglacial records of the reflectance of sediments from the Norwegian-Greenland-Iceland Sea (Nordic seas): International Journal of Earth Sciences, v. 88, p. 325-336.

Bauch, H. A., Erlenkeuser H., Fahl, K., Spielhagen R. F., Weinelt M. S., Andruleit, H., and Henrich, R., 1999, Evidence for a steeper Eemian than Holocene sea surface temperature gradient between Arctic and sub-Arctic regions: Palaeogeography, Palaeoclimatology, Palaeoecology, v. 145, p. 95-117.

Bauch, H. A., Erlenkeuser, H., Jung, S. J. A., and Thiede, J., 2000a, Surface and deep water changes in the subpolar North Atlantic during Termination II and the last interglaciation: Paleoceanography, v. 15, p. 76-84.

Bauch, H. A., Erlenkeuser, H., Helmke, J. P., and Struck, U., 2000b, A paleoclimatic evaluation of marine oxygen isotope stage 11 in the high-northern Atlantic (Nordic seas): Global and planetary change, v. 24, p. 27-39.

Bauch, H. A., Erlenkeuser, H., Spielhagen, R., Struck, U., Matthiessen, J., Thiede, J., and Heinemeier, J., 2001a, A multiproxy reconstruction of the evolution of deep and surface waters in the subarctic Nordic seas over the last 30,000 years: Quaternary Science Reviews, v. 20, p. 659-678.

Bauch, H. A., Struck, U., and Thiede, J., 2001b, Planktic and benthic foraminifera as indicators for past ocean changes in surface and deep waters of the Nordic seas, *in* Schäfer, P., Ritzrau, W., Schlüter, M., and Thiede, J., eds., The Northern North Atlantic: a changing environment., New York, Springer-Verlag, p. 411-421.

Bauch, H. A., and Erlenkeuser, H., in press, Interpreting glacial-interglacial changes in ice volume and climate from subarctic deep water foraminiferal $\delta^{18}O$, *in* Droxler A., Poore R., Burckle L., and Osterman L., eds., Earth's Climate and Orbital Eccentricity: Marine Isotope Stage 11 Question, Washington, D. C., American Geophysical Union Monograph Series.

Bé, A. W. H., and Tolderlund, D. S., 1971, Distribution and ecology of living planktonic foraminifera in surface waters of the Atlantic and Indian oceans, *in* Funnel, B. M., and Riedel, W. R., ed., The Micropaleontology of Oceans, Cambridge, Cambridge University Press, p. 105-149.

Bé, A. W. H., 1977, An ecological, zoographic and taxonomic review of recent planktonic foraminifera, *in* Ramsay, A. T. S., ed., Oceanic Micropaleontology, London, Academic Press, p. 1-100.

Bé, A. W. H., and Hutson, W. H., 1977, Ecology of planktonic foraminifera and biogeographic patterns of life and fossil assemblages in the Indian Ocean: Micropaleontology, v. 23, p. 369-414.

Berger, W. H., 1968, Planktonic Foraminifera: selective solution and paleoclimatic interpretation: Deep-Sea Research, v. 15, p. 31-43.

Berger, W. H., 1971, Sedimentation of planktonic foraminifera: Marine Geology, v. 11, p. 325-358.

Blunier, T., Chappelaz, J., Schwander, J., Dällenbach, A., Stauffer, B., Stocker, T. F., Raynaud, D., Jouzel, J., Clausen, H. B., Hammer, C. U., and Johnsen, S. J., 1998, Asynchrony of Antarctic and Greenland climate change during the last glacial period: Nature, v. 394, p. 739-743.

Bond, G., Heinrich, H., Broecker, W., Labeyrie, L., McManus, J., Andrews, J., Huon, S., Jantschik, R., Clasen, S., Simet, C. Tedesco, K., Klas, M., and Bonani,G. Ivy, S., 1992, Evidence for massive discharge of icebergs into the North Atlantic ocean during the last glacial period: Nature, v. 360, p. 245-249.

Bond, G., Broecker, W. C., Johnsen, S., McManus, J., Labeyrie, L., Jouzel, J., and Bonani, G., 1993, Correlations between climate records from North Atlantic sediments and Greenland ice: Nature, v. 365, p. 143-147.

Bond, G., 1995, Oceanography; climate and the conveyor: Nature, v. 377, p. 383-384

Bond, G. C., and Lotti, R., 1995, Iceberg discharges into the North Atlantic on millennial time scales during last glaciation: Science, v. 267, p. 1005-1010.

Bond, G. C., Showers, W., Cheseby, M., Lotti, R., Almasi, P., deMonecal, P., Priore, P., Cullen, H., Hajdas, I. and Bonani, G., 1997, A pervasive millennial-scale cycle in North Atlantic Holocene and Glacial climates: Science, v. 278, p. 1257-1266.

Broecker, W. S., and Denton, G. H., 1990, The role of ocean-atmosphere reorganizations in glacial cycles: Quaternary Science Reviews., v. 9, p. 305-341.

Broecker, W. S., 1991, The great ocean conveyor: Oceanography, v. 4, p. 79-89.

Broecker, W. S., 1994, Massive iceberg discharges as triggers for global climate change: Nature, v. 372, p. 421-424.

Broecker, W. S., 1997, Thermohaline circulation, the achilles heel of our climate system: Will man-made CO_2 upset the current balance?: Science, v. 278, p. 1582-1588.

Brown, S. J., 1996, Controls on the trace metal chemistry of foraminiferal calcite and aragonite: Ph.D. thesis, University of Cambridge, 231 p.

Brummer, G. J. A., 1988, Comparative ontogeny and species definition of planktonic foraminifers: A case study of *Dentigloborotalia anfracta* n.gen, *in* Brummer, G. J. A., and Kroon, D., eds., Planktonic foraminifers as tracers of ocean-climate history, Amsterdam, Free University Press, p. 51-71.

Campbell, I. D., Campbell, C., Apps, M. J., Rutter, N. W., and Bush, A. B. G., 1998, Late Holocene ~1500 yr. periodicities and their implications: Geology, v. 26, p. 471-473.

Carstens, J., Hebbeln, D., and Wefer, G., 1997, Distribution of planktic foraminifera at the ice margin in the Arctic (Fram Strait): Marine Micropaleontology, v. 29, p. 257-269.

Chapman, M. R., and Maslin, M. A., 1999, Low-latitude forcing of meridional temperature and salinity gradients in the subpolar North Atlantic and the growth of glacial ice sheets: Geology, v. 27, p. 875-878.

Chapman, M. R., and Shackleton, N. J., 1999, Global ice-volume fluctuations, North Atlantic ice-rafting events, and deep-ocean circulation changes between 130 and 70 ka: Geology, v. 27, p. 795-798.

Chapman, M. R., Shackleton, N. J., and Duplessy, J.-C., 2000, Sea surface temperature variability during the last glacial-interglacial cycle: assessing the magnitude and pattern of climate change in the North Atlantic: Palaeogeography, Palaeoclimatology, Palaeoecology, v. 157, p. 1-25.

Clark, P. U., Pisias, N. G., Stocker, T. F., and Weaver, A. J., 2002, The role of the thermohaline circulation in abrupt climate change: Nature, v. 415, p. 863-869.

CLIMAP MEMBERS, 1976, The surface of Ice-Age Earth: Science, v. 191, p. 1131-1137.

Dansgaard, W., Johnsen, S. J., Clausen, H. B., Dahl-Jensen, D., Gundestrup, N. S., Hammer, C. U., Hvidberg, C. S., Steffensen, J. P., Sveinbjörnsdottir, A. E., Jouzel, J. and Bond, G., 1993, Evidence for general instability of past climate from a 250-kyr ice-core record: Nature, v. 364, p. 218-220.

Darling, K. F., Kucera, M., Wade, C., Kroon, D., Dingle, R., Pudsey, C., Brinkmeyer, R., Bauch, D., and Stangeew, E., 2001, Unravelling the genetic relationships between the bipolar high latitude populations of the planktonic foraminifer *Neogloboquadrina pachyderma* sin.: International Conference on Paleoceanography (ICP-VII), p.95.

Davis, J. C., 1986, Statistics and data analysis in geology: New York, John Wiley, 646 p.

de Menocal, P., Ortiz, J. D., Guilderson, T., and Sarnthein M., 2000, Coherent high- to low-latitude climate variability during the Holocene warm period: Science, v. 288, p. 2198-2202.

Deuser, W. G., and Ross, E. H., 1989, Seasonally abundant planktonic foraminifera of the Sargasso Sea: Succession, deep-water fluxes, isotopic compositions, and paleoceanographic implications: Journal of Foraminiferal Research, v. 19, p. 268-293.

de Vargas, C., Renaud, S., Hilbrecht, H., and Pawlowski, J., 2001, Pleistocene adaptive radiation in *Globorotalia truncatulinoides*: genetic, morphologic, and environmental evidence: Paleobiology, v. 27, p. 104-125.

Didié, C., and Bauch, H. A., 2000, Species composition and glacial-interglacial variations in the ostracode fauna of the northeast Atlantic during the past 200,000 years: Marine Micropaleontology, v. 40, p. 105-129.

Didié, C., Bauch, H.A. and Helmke, J.P., 2002. Late Quaternary deep-sea ostracodes in the polar and subpolar North Atlantic: paleoecological and paleoenvironmental implications. Palaeogeography, Palaeoclimatology, Palaeoecology, v. 184 p.195-212.

Didié, C., Bauch, H. A., and Helmke, J. P., 2002, Late Quaternary deep-sea ostracodes in the polar and subpolar North Atlantic: paleoecological and paleoenvironmental implications: Palaeogeography, Palaeoclimatology, Palaeoecology, v. 184, p. 195-212.

Dokken, T. M., and Hald, M., 1996, Rapid climatic shifts during isotope stages 2-4 in the Polar North Atlantic: Geology, v. 24, p. 599-602.

Dowsett, H. J., and Poore, R. Z., 1990, A new planktic foraminifer Transfer Function for estimating Pliocene-Holocene paleoceanographic conditions in the North Atlantic: Marine Micropaleontology, v. 16, p. 1-23.

Elderfield, H., and Ganssen, G., 2000, Past temperature and $\delta^{18}O$ of surface ocean waters inferred from foraminiferal Mg/Ca ratios: Nature, v. 405, p. 442-445.

Elliot, M., Labeyrie, L., Bond, G., Cortijo, E., Turon, J. L., Tisnerat, N., and Duplessy, J.-C., 1998, Millennial-scale iceberg discharges in the Irminger Basin during the last glacial period: Relationship with the Heinrich events and environmental settings: Paleoceanography, v. 13, p. 433-446.

Fronval, T., and Jansen, E., 1996, Rapid changes in ocean circulation and heat flux in the Nordic seas during the last interglacial period: Nature, v. 383.

Ganopolski, A., and Rahmstorf, S., 2001, Rapid changes of glacial climate simulated in a coupled climate model: Nature, v. 409, p. 153-158.

Ganssen, G., and Sarnthein, M., 1983, Stable-isotope composition of foraminifers: the surface and bottom water record of coastal upwelling, *in* Suess, E., and Thiede, J., eds., Responses of the sedimentary regime to present coastal upwelling, New York, London, Plenum Press, 99-121.

Grootes, P. M., Stuiver, M., White, J. W. C., Johnsen, S., and Jouzel, J., 1993, Comparison of the oxygen isotope records from the GISP 2 and GRIP Greenland ice cores: Nature, v. 366, p. 552-554.

Grootes, P. M., and Stuiver, M., 1997, Oxygen 18/16 variability in Greenland snow and ice with 10^{-3} to 10^{-5}-year time resolution: Journal of Geophysical Research, v. 102, p. 26,455-26,470.

Grousset, F. E., Labeyrie, L., Sinko, J. A., Cremer, M., Bond, G., Duprat, J., Cortijo, E. and Huon, S., 1993, Patterns of ice-rafted detritus in the glacial North Atlantic (40°-55°N): Paleoceanography, v. 8, p. 175-192.

Gwiazda, R. H., Hemming, S. R., and Broecker, W. S., 1996, Provenance of icebergs during Heinrich event 3 and the contrast to their sources during other Heinrich events: Paleoceanography, v. 11, p. 371-378.

Hale, W., and Pflaumann, U., 1999, Sea-Surface Temperature Estimations Using a Modern Analog Technique with Foraminiferla Assembleages from Western Atlantic Quaternary Sediments, *in* Fischer, G., and Wefer, G., eds., Use of proxies in paleoceanography, Berlin, Springer, p. 69-90.

Haug, G. H., and Tiedemann, R., 1998, Effect of the formation of the Isthmus of Panama on Atlantic Ocean thermohaline circulation: Nature, v. 393, p. 673-676.

Hays, J. D., Imbrie, J., and Shackleton, N. J., 1976, Variations in the earth's orbit: pacemaker of the Ice Age: Science, v. 194, p. 1121-1132.

Healy-Williams, N., 1992, Stable isotope differences among morphotypes of *Neogloboquadrina pachyderma* (Ehrenberg): Implications for high-latitude palaeoceanographic studies: Terra Nova, v. 4, p. 693-700.

Hebbeln, D., Dokken, T., Andersen, E. S., Hald M. and Elverhoi A., 1994, Moisture supply for northern ice-sheet growth during the Last Glacial Maximum: Nature, v. 370, p. 357-360.

Heinrich, H., 1988, Origin and consequences of cyclic ice-rafting in the northeast Atlantic Ocean during the past 130,000 years: Quaternary Research, v. 29, p. 142-152.

Helmke, J. P., and Bauch, H. A., 2001, Glacial-interglacial relationship between carbonate components and sediment reflectance in the North Atlantic: Geo-Marine Letters, v. 21, p. 16-22.

Helmke, J. P., Sculz, M., and Bauch, H. A., 2002, Sediment color record reveals patterns of millennial-scale climate variability over the last 500,000 years: Quaternary Research, v. 57, p. 16-22.

Helmke, J. P., and Bauch, H. A., submit., Comparison of glacial and interglacial conditions between the polar and subpolar North Atlantic Region over the last five climatic cycles: Paleoceanography.

Hemleben, C., Spindler, M., and Anderson, O. R. 1989, Modern Planktonic Foraminifera: New York, Springer, 365 p.

Herman, Y., 1972, *Globorotalia truncatulinoides*: a palaeo-oceanographic indicator: Nature, v. 238, p. 394-396.

Howard, W. R., 1997, A warm future in the past: Nature, v. 388, p. 418-419.

Hüls, M., and Zahn, R., 2000, Millennial-scale sea surface temperature variability in the western tropical North Atlantic from planktonic foraminiferal census counts: Paleoceanography, v. 15, p. 659-678.

Hutson, W. H., 1980, The Agulhas current during the late Pleistocene: Analysis of modern faunal analogs: Science, v. 207, p. 64-66.

Imbrie, J., and Kipp, N. G., 1971, A new micropaleontological method for quantitative paleoclimatology: Application to a Late Pleistocene Caribbean core, *in* Turekian, K. K., ed., The Late Cenozoic Glacial Ages, New Haven, London, Yale University Press, p. 71-181.

Jansen, E., and Veum, T., 1990, Evidence for two-step deglaciation and its impact on North Atlantic deep-water circulation: Nature, v. 343, p. 612-616.

Johannessen, M., 1986, Brief overview over the physical oceanography, *in* Hurdle, B. G., ed., The Nordic Seas, New York, Springer Verlag, p. 103-128.

Johannessen, T., Jansen, E., Flatoy, A., and Ravelo, A. C., 1994, The relationship between surface water masses, oceanographic fronts and paleoclimatic proxies in surface sediments of the Greenland, Iceland, Norwegian Seas, *in* Zahn, R., Pedersen, T. F., Kaminski, M. A., and Labeyrie, L., eds., Carbon Cycling in the Glacial Ocean: Constrains of the Oceans's Role in Global Change, Berlin, Springer, p. 61-85.

Johnsen, S. J., Clausen, H. B., Dansgaard, W., Fuhrer, K., Gundestrup, N., Hammer, C. U., Iversen, P., Jouzel, J., Stauffer, B. and Steffensen, J. P., 1992, Irregular glacial interstadials recorded in a new Greenland ice core: Nature, v. 359, p. 311-313.

Jung, S. J. A., 1996, Wassermassenaustausch zwischen NE-Atlantik und Nordmeer während der letzten 300.000/80.000 Jahre im Abbild stabiler O- und C-Isotope: Berichte SFB 313, University of Kiel, v. 61, 104 p.

Kandiano, E. S., and Bauch, H. A., 2002, Implications of planktic foraminiferal size fractions for the glacial-interglacial paleoceanography of the polar North Atlantic: Journal of Foraminiferal Research, v 32, p. 245-251.

Kellogg, T. B., 1976, Late Quaternary climatic changes: evidence from deep-sea cores of Norwegian and Greenland Seas, *in* Cline, R. M., and Hays, J. D., eds., Investigation of Late Quaternary Paleoceanography and Paleoclimatology, Boulder, Geological Society of America Memoir, v. 145, p. 77-110.

Kellogg, T. B., 1977, Paleoclimatology and paleo-oceanography of the Norwegian and Greenland Seas: The last 450,000 yeras: Marine Micropaleontology, v. 2, p. 235-249.

Kellogg T. B., 1980, Paleoclimatology and paleo-oceanography of the Norwegian and Greenland Seas: glacial-interglacial contrasts: Boreas, v. 9, p. 5-37.

Kellogg T. B., 1984, Paleoclimatic significance of subpolar foraminifera in high-latitude marine sediments: Canadian Journal of Earth Science, v. 21, p. 189-193.

Kennett, J. P., and Srinivasan, M. S., 1983, Neogene planktonic foraminifera - A philogenetic atlas: Stroudsburg, Pennsylvania, Hutchinson Ross Publishing Company, 263 p.

Kipp, N., 1976, New transfer function for estimating past sea surface conditions from sea bed distribution of planktonic foraminiferal assemblages in the North Atlantic, *in* Cline, R. M., and Hays, J. D., eds., Investigation of Late Quaternary Paleoceanography and Paleoclimatology, Boulder, Geological Society of America Memoir, v. 145, p. 3-41.

Klovan, J. E., and Imbrie, J., 1971, An Algorithm and Fortran IV Program for Large-Scale Q-Mode Factor Analysis and Calculation of Factor Scores: Mathematical Geology, v. 3, p. 61-77.

Kotilainen, A. T., and Shackleton, N. J., 1995, Rapid climate variability in the North Pacific Ocean during the past 95,000 years: Nature, v. 377, p. 323-326.

Kroon, D., Wouthers, P., Moodley, L., Ganssen, G., and Troelstra, S. R., 1988, Phenotypic variation of *Turborotalita quinqueloba* (Natland) tests in living populations and in the Pleistocene of an eastern Mediterranean piston core, *in* Brummer, G. J. A., and Kroon, D., eds., Planktonic foraminifers as tracers of ocean-climate history, Amsterdam, Free University Press, p. 131-143.

Kuehnen, E. C., Alvarez, R., Paulson, P.J., and Murphy, T. J., 1972, Production and analysis of special high purity acids purified by sub-boiling distillation: Analytical Chemistry v. 44, p. 2050-6.

Le, J., and Shackleton, N. J., 1994, Reconstructing paleoenvironment by transfer function: model evaluation by simulated data: Marine Micropaleontology, v. 24, p. 187-199.

Le, J., and Thunell, R. C., 1996, Modeling planktic foraminiferal assemblage changes and application to surface temperature estimation in the western equatorial Pacific ocean: Marine Micropaleontology, v. 28, p. 211-229.

Lee, K. E., and Slowey, N. C., 2001, Glacial sea surface temperatures in the subtropical North Pacific: A comparison of $U^{k'}_{37}$, $\delta^{18}O$, and foraminiferal temperature estimates: Paleoceanography, v. 16, p. 268-279.

Levitus, S., and Boyer, T. P., 1994, World Ocean Atlas 1994: Temperature, NOAA Atlas NESDIS 4: Washington, D.C., Department of Commerce, 117 p.

Lototskaya, A., Ziverti P., Ganssen, G. M., and van Hinte, J. E., 1998, Calcareous nannofloral response to Termination II at 45°N, 25°W (northeast Atlantic): Marine Micropaleontology, v. 34, p. 47-70.

Lototskaya, A., and Ganssen, G. M., 1999, The structure of Termination II (penultimate deglaciation and Eemian) in the North Atlantic: Quaternary Science Reviews, v. 18, p. 1641-1654.

Loubere, P., 1981, Oceanographic parameters reflected in the seabed distribution of planktic foraminifera from the North Atlantic and Mediterranean sea: Journal of Foraminiferal Research, v. 11, p. 137-158.

Lowell, T. V., Heusser, C. J., Andersen, B. G., Moreno, P. I., Hauser, A., Heusser, L. E., Schluchter, C., Marchant, D. R., and Denton, G. H., 1995, Interhemispheric correlation of late Pleistocene glacial events: Science, v. 269, p. 1541-1549.

Lyle, M., Heusser, L., Herbert, T., Mix, A., and Barron, J., 2001, Interglacial theme and variations: 500 k.y. of orbital forcing and associated responses from the terrestrial and marine biosphere, U.S. Pacific Northwest: Geology, v. 29, p. 1115-1118.

Malmgren, B. A., Kennett, J. P., 1976, Test size variations in *Globigerina bulloides* in response to Quaternary palaeoceanographic changes: Nature, v. 275, p. 123-124.

Manigetti, B., and McCave, I. N., 1995, Late glacial and Holocene palaeocurrents around Rackall Bank, NE Atlnatic Ocean: Paleoceanography, v. 10, p. 611-626.

Marotzke, J., 2000, Abrupt climate change and thermohaline circulation: Mechanisms and predictability: PNAS, v. 97, p. 1347-1350.

Marquard, R. S., and Clark, D. L., 1987, Pleistocene paleoceanographic correlations: Northern Greenland Sea to central Arctic Ocean: Marine Micropaleontology, v. 12, p. 325-341.

Martinson, D. G., Pisias, N. G., Hays, J. D., Imbrie, J., Moore, T. C., and Shackleton, N. J., 1987, Age dating and the orbital theory of the Ice Ages: Development of a high-resolution 0 to 300,000-year chronostratigraphy: Quaternary Research, v. 27, p. 1-29.

Mashiotta, T. A., Lea, D. W., and Spero, H. J., 1999, Glacial-interglacial changes in Subantarctic sea surface temperature and δ^{18}O-water using foraminiferal Mg: Earth and Planetary Science Letters, v. 170, p. 417-432.

Maslin, M. A., and Shackleton, N.J., 1995, Surface water temperature, salinity, and density changes in the northeast Atlantic during the last 45,000 years: Heinrich events, deep water formation, and climatic rebounds: Paleoceanography, v. 10, p. 527-544.

Maslin, M., Seidov, D., and Lowe, J., 2001, Synthesis of the Nature and Causes of Rapid Climate Transitions During the Quaternary, *in* Seidov, D., Haupt, P. J. and Maslin, M., eds., The Oceans and Rapid Climate Change: Past, Present, and Future, Washington D.C., American Geophysical Union, p. 9-51.

Mauritzen, C., 1996, Production of dense overflow waters feeding the North Atlantic across the Greenland-Scotland Ridge. Part 1: Evidence for a revised circulation scheme: Deep-Sea Research, v. 43, p. 769-806.

McCave, I. N., and Tucholke, B. E., 1986, Deep current-controlled sedimentation in the western North Atlantic, *in* Vogt, P. R., and Tucholke, B. E., eds., The Geology of North America, Boulder, Geological Society of America Memoir, p. 451-468.

McIntyre, A., Ruddiman, W. F., and Jantzen, R., 1972, Southward penetrations of the North Atlantic Polar Front; faunal and floral evidence of large-scale surface water mass movements over the last 225,000 years: Deep-Sea Research, v. 19, p. 61-77.

McIntyre, A., Ruddiman, W. F., Karlin, K., and Mix, A. C., 1989, Surface water response of the Equatorial Atlantic ocean to orbital forcing: Paleoceanography, v. 4, p. 19-55.

McManus, J. F., Bond, G. C., Broecker, W. S., Johnsen, S., Labeyrie, L. and Higgins, S., 1994, High-resolution climate records from the North Atlantic during the last interglacial: Nature, v. 371, p. 326-329.

McManus, J. F., Oppo, D. W., and Cullen, J. L., 1999, A 0.5-Million-Year Record of Millennial-Scale Climate Variability in the North Atlantic: Science, v. 283, p. 971-975.

Mekik, F., and Loubere, P., 1999, Quantitative paleo-estimation: hypothetical experiments with extrapolation and the no-analog problem: Marine Micropaleontology, v. 36, p. 225-248.

Mix, A. C., and Morey, A. E., 1996, Climate Feedback and Pleistocene variations in the Atlantic South Equatorial Current., *in* Wefer, G., Berger, W. H., Siedler, G., and Webb, D. J., eds., The South Atlantik: Present and Past Circulation, Berlin, Springer, p. 503-525.

Mix, A. C., Morey, A. E., Pisias, N. G., and Hostetler, S. W., 1999, Foraminiferal faunal estimates of paleotemperature: Circumventing the no-analog problem yields cool ice age tropics: Paleoceanography, v. 14, p. 350-359.

Molfino, B., Kipp, N. G., and Morley, J. J., 1982, Comparison of foraminiferal, coccolithophorid and radiolarian paleotemperature equations: Assemblage coherency and estimate concordancy: Quaternary Research, v. 17, p. 279-313.

Mulitza, S., Dürkoop, A., Hale, W., Wefer, G., and Niebler, H. S., 1997, Planktonic foraminifera as recorders of past surface-water stratification: Geology, p. 335-338.

Müller, A., 2000, Mg/Ca and Sr/Ca-Verhältnisse in biogenem carbonat planktischer Foraminiferen und bentischer Ostracoden: Berichte aus dem Institut für Meereskunde 313, University of Kiel, 182 p.

Niebler, H.-S., and Gersonde, R., 1998, A planktic foraminiferal transfer function for the southern South Atlantic Ocean: Marine Micropaleontology, v. 34, p. 213-234.

Niscott, R. N., Aksu, A. E., Mudie, P. J., and Parsons, D. F., 2001, A 340,000 year record of ice rafting, palaeoclimatic fluctuations, and shelf-crossing glacial advances in the southwestern Labrador Sea: Global and Planetary Change, v. 28, p. 227-240.

Nürnberg, D., Bijma, J., and Hemleben, C., 1996, Assessing the reliability of magnesium in foraminiferal calcite as a proxy for water mass temperatures: Geochimica et cosmochimica Acta, v. 60, p. 803-814.

Nürnberg, D., Müller, A., and Schneider, R. R., 2000, Paleo-sea surface temperature calculations in the eaquatorial east Atlantic from Mg/Ca ratios in planktic foraminifers: A comparison to SST estimates from $U^{K'}37$ and transfer function: Paleoceanography, v. 15, p. 124-134.

Oppo, D. W., and Lehmann, S. J., 1995, Suborbital timescale variability of North Atlantic Deep Water during the past 200,000 years: Paleoceanography, v. 10, p. 901-910.

Oppo, D. W., McManus, J. F., and Cullen, J. L., 1998, Abrupt climatic events 500,000 to 340,000 years ago: Evidence from subpolar North Atlantic sediments: Science, v. 297, p. 1335-1338.

Oppo, D. W., Keigwin, L.D., and McManus, J. F., 2001, Persistent suborbital climate variability in marine isotope stage 5 and Termination II: Paleoceanography, v. 16, p. 280-292.

Ortiz, J. D., and Mix, A. C., 1997, Comparison of Imbrie-Kipp transfer function and modern analog temperature estimates using sediment trap and core top foraminiferal faunas: Paleoceanography, v. 12, p. 175-190.

Ottens, J. J., 1992, Planktic foraminifera as indicators of ocean environments in the northeast Atlantic: Ph.D. thesis, University of Amsterdam, 189 p.

Overpeck., J. T., Webb III, T., and Prentice, I. C., 1985, Quantitative Interpretation of Fossil Pollen Spectra: Dissimilarity Coefficients and the Method of Modern Analogs: Quaternary Research, v. 23, p. 87-108.

Paillard, D., and Cortijo, E., 1999, A simulation of the Atlantic meridional circulation during Heinrich event 4 using reconstructed sea surface temperatures and salinities: Paleoceanography, v. 14, p. 716-724.

Parker, F., and Berger, W. H., 1971, Faunal and solution patterns of planktonic foraminifera in surface sediments of the South Pacific: Deep-Sea Research, v. 18, p. 73-107.

Peeters, F., Ivanova, E., Conan, S., Brummer G. J., Ganssen, G., Troelstra, S., and Hinte, J., 1999, A size analysis of planktic foraminifera from the Arabian Sea: Marine Micropaleontology, v. 36, p. 31-63.

Pflaumann, U., Duprat, J., Pujol, C., and Labeyrie, L. D., 1996, SIMMAX: A modern analog technique to deduce Atlantic sea surface temperatures from planktonic foraminifera in deep-sea sediments: Paleoceanography, v. 11, p. 15-35.

Prell, W. L., and Curry, W. B., 1981, Faunal and isotopic indexes of monsoonal upwelling: Western Arabian Sea: Oceanologica Acta, v. 4, p. 91-98.

Prell, W. L., 1985, The stability of low latitude sea surface temperatures: An evaluation of the CLIMAP reconstruction with emphasis on positive SST anomalies, Rep. TR 025, Washington D.C., Dept. of Energy, 60 p.

Puechmaille, C., 1994, Mg, Sr and Na fluctuations in the test of modern and recent *Globigerina bulloides*: Chemical Geology, v. 116, p. 147-152.

Rahmstorf, S. 1994, Rapid climate transitions in a coupled ocean-atmosphere model: Nature, v. 372, p. 82-85.

Rahmstorf, S., 1995, Bifurcations of the Atlantic thermohaline circulation in response to changes in the hydrological cycle: Nature, v. 378, p. 145-149.

Rahmstorf, S., 1996, On the freshwater forcing and transport of the Atlantic thermohaline circulation: Climate Dynamics, v. 12, p. 799-811.

Rasmussen, T. L., van Weering, T. C. E., and Laberyrie, L., 1997, Climatic instability, ice sheets and ocean dynamics at high northern latitudes during the last glacial period (58-10 ka BP): Quaternary Science Reviews, v. 16, p. 73-80

Rohling, E. J., Fenton, M., Jorissen, F. J., Bertrand, P., Ganssen, G., and Caulet, J. P., 1998, Magnitudes of sea-level lowstands of the past 500,000 years: Nature, v. 394, p. 162-165.

Ruddiman, W. F., and McIntyre, A., 1976, Northeast Atlantic paleoclimatic changes over the past 600,000 years, *in* Cline, R. M., and Hays, J. D., eds., Investigation of Late Quaternary Paleoceanography and Paleoclimatology, Boulder, Geological Society of America Memoir, v. 145, p. 155-173.

Ruddiman, W. F., 1977, Late Quaternary deposition of ice-rafted sand in the subpolar North Atlantic (lat. 40° to 65°N): Geological Society of America Bulletin, v. 88, p. 1813-1821.

Ruddiman, W. F., and McIntyre, A., 1984, Ice-age thermal response and climatic role of the surface Atlantic Ocean, 40°N to 63°N: Geological Society of America Bulletin, v. 95, p. 381-396.

Ruddiman, W. F., Raymo, M. E., and McIntyre, A., 1986a, Matuyama 41,000-year cycles: North Atlantic Ocean and northern hemisphere ice sheets: Earth and Planetary Science Letters, v. 80, p. 117-129.

Ruddiman, W. F., Shackleton, N. J., and McIntyre, A., 1986, North Atlantic sea-surface temperatures for the last 1,1 million years, *in* Summerhayes, C. P., and Shackleton, N. J., eds., North Atlantic paleoceanography, Boulder, Geological Society Special Publication, p. 155-173.

Ruddiman, W. F., and Esmay, A., 1987, A streamlined foraminiferal transfer function for the subpolar North Atlantic: Initial reports of the Deep Sea Drilling Project, v. 94, p. 1045-1057.

Saito, T., Thompson, P. R., and Breger, D., 1981, Systematic index of recent and Pleistocene planktonic foraminifera: Tokyo, University of Tokyo Press, 190 p.

Sarnthein, M., and Tiedemann, R., 1990, Younger Dryas-style cooling events at glacial terminations I-VI at ODP Site 658; associated benthic $\delta^{13}C$ anomalies constrain meltwater hypothesis: Paleoceanography, v. 5, p. 1041-1055.

Sarnthein, M., Stattegger, K., Dreger, D., Erlenkeuser, H., Grootes, P., Haupt, B. J., Jung, S., Kiefer, T., Kuhnt, W., Pflaumann, U., Schäfer-Neth, C., Schulz, H., Schulz, M., Seidov, D., Simstich, J., van Kreveld, S., Vogelsang, E., Völker, A., and Weinelt, M., 2001, Fundamental Modes and Abrupt Changes in North Atlantic Circulation and Climate over the last 60 ky - Concepts, Reconstruction and Numerical Modeling,

in Schäfer, P., Ritzrau, U., Schlüter, M., and Thiede, J., eds., The Northern North Atlantic: A Changing Environment, Berlin, Springer, p. 365-410.

Schott, W., 1935, Die Foraminiferen aus dem aequatorialen Teil des Atlantischen Ozeans, Deutsch. Atlant. Exped. "Meteor" 1925-1927, Wissenschaftliche Ergebnisse, p. 43-134.

Schulz, H., 1994, Meeresoberflächentemperaturen im Nordatlantik und in der Norwegish-Grönländischen See vor 9000 Jahren. Auswirkungen des frühholozäanen Insolationsmaximums: Ph.D. thesis, University of Kiel, 119 p.

Schulz, H., von Rad, U., and Erlenkeuser, H., 1998, Correlation between Arabian Sea and Greenland climate oscillations of the past 110,000 years: Nature, v. 393, p. 54-57.

Seidov, D., and Maslin, M., 1999, North Atlantic deep water circulation collapse during Heinrich events: Geology, v. 27, p. 23-26.

Shackleton, N. J., 2000, The 100,000-year ice-age cycle identified and found to lag temperature, carbon dioxide, and orbital eccentricity: Science, v. 289, p. 1989-1902.

Suess, E., and Altenbach, A. V., 1992, Europäisches Nordmeer, Reise Nr. 17, 15. Juli-29. August 1991: METEOR-Berichte, University of Hamburg, v. 92-3, p. 1-164.

van Kreveld, S., Sarnthein, M., Erlenkeuser, H., Grootes, P., Jung, S., Nadeau, M. J., Pflaumann, U., and Voelker, A., 2000, Potential links between surging ice sheets, circulation changes, and the Dansgaard-Oeschger cycles in the Irminger Sea, 60-18 kyr: Paleoceanography, v. 15, p. 425-442.

Vincent, E., and Berger, W. H., 1981, Planktonic foraminifera and their use in Paleoceanography, *in* Emiliani, C., ed., The Sea, The Oceanic Lithosphere, New York, Wiley, p. 1025-1118.

Wadhams, P., 1986, The ice cover, *in* Hurdle, B.G. (ed.), The Nordic Seas, New York, Springer-Verlag, p. 20-84.

Waelbroeck, C., Labeyrie, L., Duplessy, J.-C., Guiot, J., Labracherie, M., Leclaire, H., and Duprat, J., 1998, Improving past sea surface temperature estimates based on planktonic fossil faunas: Paleoceanography, v. 13, p. 272-283.

Wang, L., Sarnthein, M., Pflaumann, U., Heilig, S., Kienast, M., Ivanova, E., Erlenkeuser, H., Grootes, P., Grimalt, J. O., and Pelejero, C., 1999, East Asian monsoon climate during the late Pleistocene: High resolution sediment records from the South China Sea: Marine Geology, v. 156, p. 245-284.

Weinelt, M., Sarnthein, M., Pflaumann, U., Schulz H., Jung, S., and Erlenkeuser, H., 1996, Ice-free Nordic seas during the last glacial maximum? Potential sites of deepwater formation: Palaeoclimates, v. 1, p. 283-309.

Winograd, I. J., Tyler, B. C., Landwehr, J. M., Riggs, A. C., Ludwig, K. R., Szabo, B. J., Kolesar, P. T. and Revesz, K. M., 1992, Continuous 500,000-year climate record from vein calcite in Devils Hole, Nevada: Science, v. 258, p. 255-260.

Zhao, M., Beveridge, N. A. S., Shackleton, N. J., Sarnthein, M., and Eglinton, G., 1995, Molecular stratigraphy of cores off northwest Africa: Sea surface temperature history over the last 80 ka: Paleoceanography, v. 10, p. 661-675.

Acknowledgments

I would like to thank Prof. Dr. Christian Dullo for his encouragement and supervision of this work. My special thanks go to my supervisor Dr. Henning Bauch who was guiding me in science, discussing with me all aspects of my work, and correcting my numerous "draft versions". Without his never-ending criticism this work would be much poorer as well as daily life in general.

I am gratefully acknowledge financial support of the DFG in the form of a stipend in the graduate school project "Dynamics of Global Cycles within the System Earth" (Kiel University). The final step of the work was supported from the personal Leibniz award to Prof. Dr. Dullo.

I also should express my gratitude to Dr. Matthias Hüls for the first introduction to mathematical approaches of sea surface temperature estimations, help with literature and fruitful scientific comments.

Dr. Henning Bauch and Dr. Pflaumann helped me to elaborate my foraminiferal taxonomy. Dr. Jan Helmke and Dr. Anja Müller shared with me some data generated during their Ph.D. studies. I have also benefited from scientific discussions with Akad. Lisitsyn, Dr. M. Barash, Dr. Dmitrenko, S. Kirillov and G. Bozzano. Dr. E. Taldenkova needs to be mentioned because she was often the first who had to read my English manuscripts.

I give my thanks to Karen Volkmann-Lark for help with translation "Abstract" into German language.

My thanks are also given to Angelika Finke for very well-organized library facilities at GEOMAR.

I am also grateful for the good organization within the graduate school, the useful seminars and excursions, as well as to all my graduate colleagues, first of all to Dr. Michael Abratis whose carrying attitude was extended to all our problems related to work and social life.

My thanks also go to all colleagues engaged in the Laptev Sea project, "Russian-German family", for share lots of long evenings doing work and having fun, and for the warm "home" atmosphere that I was enjoying as a member of this "familiy".

My friends in Kiel, the Gurenkos, the Portnyagins, Nadja Svetlova, and Heiko Klotz, I thank for sharing my light and dark days.

My deep thanks I express to my relatives the Schleichers who helped me with all daily-life problems during these three years.

Appendix*

Table A.1. M23414, Planktic foraminiferal census data.

Table A.2. M23414 temperatures estimated with MAT method during MIS 1-13 (data base consists 738 core tops).

Table A.3. M23414, temperature estimated with MAT and TFT metods and factors derived from TFT during MIS 1-7 (data base consists of 721 core tops).

Table A.4. PS1243, foraminiferal census data for MIS 7; fraction 80-150 µm.

Table A.5. PS1243, foraminiferal census data for MIS 7; fraction100-150 µm.

Table A.6. PS1243, foraminiferal census data for MIS 7; fraction125-250 µm.

Table A.7. PS1243, foraminiferal census data for MIS 7; fraction 150-500 µm.

Table A.8. PS1243, foraminiferal census data for MIS 1-3; fraction 80-150 µm.

Table A.9. PS1243, foraminiferal census data for MIS 1-3; fraction125-250 µm.

Table A.10. PS1243, foraminiferal census data for MIS 1-3; fraction150-500 µm.

Table A.11. PS1243, test fragments for MIS 7; fraction 150-500 µm.

Table A.12. PS1243, test fragments for MIS 1-3; fraction 150-500 µm.

Table A.13. PS 1243, planktic stable oxygen isotope data.

*URL: http:www.pangaea.de/PangaVista?query=@Ref23638